Calculation of the self-consistent current distribution and coupling of an RF antenna array

Marc Ballico and Satish Puri

IPP 4/263 October 1993

MAX-PLANCK-INSTITUT FÜR PLASMAPHYSIK

85748 GARCHING BEI MÜNCHEN

MAX-PLANCK-INSTITUT FÜR PLASMAPHYSIK
GARCHING BEI MÜNCHEN

Calculation of the self-consistent current distribution and coupling of an RF antenna array

Marc Ballico and Satish Puri

IPP 4/263 October 1993

Die nachstehende Arbeit wurde im Rahmen des Vertrages zwischen dem Max-Planck-Institut für Plasmaphysik und der Europäischen Atomgemeinschaft über die Zusammenarbeit auf dem Gebiete der Plasmaphysik durchgeführt.

Calculation of the self consistent current distribution and coupling of an RF antenna array

Mark Ballico Satish Puri

October 29, 1991

Abstract

A self-consistent calculation of the antenna current distribution and fields in an axisymmetric cylindrical geometry for the ICRH antenna-plasma coupling problem is presented. Several features distinguish this calculation from other codes presently available.

1. Variational form : The formulation of the self consistent antenna current problem in a variational form allows good convergence and stability of the algorithm.
2. Multiple straps : Allows modelling of (a) the current distribution across the width of the strap (by dividing it up into sub straps) (b) side limiters & septum (c) antenna cross-coupling.
3. Analytic calculation of the antenna field and calculation of the antenna self-consistent current distribution, (given the surface impedance matrix) gives rapid calculation.
4. Framed for parallel computation on several different parallel architectures (as well as serial) gives a large speed improvement to the user.

Results are presented for both Alfvén wave heating and current drive antenna arrays, showing the optimal coupling to be achieved for toroidal mode numbers $8 < n < 10$ for typical ASDEX upgade plasmas. Simulations of the ASDEX upgrade antenna show the importance of the current distribution across the antenna and of image currents flowing in the side limiters, and an analysis of a proposed asymmetric ITER antenna is presented.

Contents

1 Introduction

There were several motivations for the development of this theory and its implementation in a computer program.

1. Present tokamaks have ICRH antennas with a physical size of the same order as the vacuum wavelength. The Faraday shield acts as an additional capacitive load to the antenna strap, making it into a slow wave structure (typically up to a factor of 2), further decreasing wavelength along the antenna strap. For example the ICRH antennas on ASDEX upgrade are $\lambda/2$ resonant at 70 MHz, and the operating frequency for 2nd harmonic Hydrogen is 60 MHz. For the next generation of tokamaks these problems become more severe, eg. for ITER the axial magnetic field is, at 6 T twice that of AUG, and the corresponding ion harmonics are at twice the frequency. The larger plasma also requires more heating, meaning a larger antenna surface. This makes it essential to correctly model the current distribution along the antenna central conductor.

2. The proposed use of ICR frequency range waves for current drive, requires that the ratio between current drive and heating be as large as possible, to keep the proportion of circulating power in a reactor as small as possible. This requires a narrow and directed spectrum of launched power, which requires an array of closely spaced antennas. For fast wave current drive scenarios, the poorer wave absorbsion (compared to minority or mode conversion heating) results in close coupling of the elements in such an array. The calculation of coupling must then be done fully self-consistently. The calculation of a cross coupling matrix for the elements is essential for the design of the feeding circuit for such an array, where some elements radiate and some absorb power.

3. The presence in real machines of non-ideal structures such as side walls in the antenna box, antenna strap separating septums and antenna protection limiters gives rise to possibly large eddy currents in these structures. These currents have the effect of changing the electrical characteristics of the antenna structure, such as the resonant frequency, as well as affecting the antenna coupling and launched power spectrum, typically putting more power than expected into high axial wavenumber modes, and reducing the antenna loading.

The calculation presented here gives the current distribution on a number of antenna loops and sources placed in a vacuum layer between the plasma edge and the vessel wall. These loops can be placed to simulate a realistic antenna structure.

The calculation may be convieniently broken up into several sections.

1. The calculation of the plasma surface impedance matrix: The wave equation is Fourier decomposed in the toroidal and poloidal directions and the resulting equation is integrated radially using a variational procedure and cubic-hermite polynomials.

2. The electromagnetic field of an arbitary current distibution on a loop: The total field of an arbitary current distribution is calculated by first computing the field for each Fourier mode, matching to the boundary conditions at the plasma surface, wall and Faraday screen. The inhomogeneous wave equation resulting from the radial volume currents within the antenna is solved analyticaly by a power series. The modes are then summed with the appropriate phase factor, to get the field at the desired point.

3. Calculation of the matrix of partial impedances: The inner product with appropriate test functions of the electric field generated by currents in each loop is calculated analyticaly.

4. Calculation of the self-consistent antenna current distribution: The source conditions at the slice generators on each loop and the boundary condition for the tangential electric field are combined with a variational form to give a system of linear equations for the unknown current distribution, and then solved.

The technique used for parallelization of the code will also be discussed.

2 Definition of dimensionless units

It is better to work in a system of units in which the Maxwell's equations reduce to a particularly simple form. The S.I. units for several quantities to be used are;

Quantity	Units	Basic Units
Z	$\Omega = \mathrm{V.A^{-1}}$	$\mathrm{kg.m^2.A^{-2}.s^{-3}}$
U	V	$\mathrm{kg.m^2.s^{-3}.A^{-1}}$
E	$\mathrm{V.m^{-1}}$	$\mathrm{kg.m.A^{-1}.s^{-3}}$
B	T	$\mathrm{kg.A^{-1}.s^{-2}}$
J	$\mathrm{A.m^{-2}}$	$\mathrm{A.m^{-2}}$
ω	$\mathrm{s^{-1}}$	$\mathrm{s^{-1}}$
μ_0	$\mathrm{H.m^{-1}}$	$\mathrm{kg.A^{-2}.s^{-2}.m}$
c	$\mathrm{m.s^{-1}}$	$\mathrm{m.s^{-1}}$
L	$\mathrm{H{=}V.s.A^{-1}}$	$\mathrm{kg.m^2.A^{-2}.s^{-2}}$
ρ	Ω.m	$\mathrm{kg.m^3.A^{-2}.s^{-3}}$

We want a system of units where ω, μ_0 and c are unity.

$$\begin{aligned} 1(\hat{\mathrm{s}}^{-1}) &= \omega(\mathrm{s}^{-1}) \\ 1(\hat{\mathrm{kg}}.\hat{\mathrm{A}}^{-2}.\hat{\mathrm{s}}^{-2}.\hat{\mathrm{m}}) &= \mu_0(\mathrm{kg.A^{-2}.s^{-2}.m}) \\ 1(\hat{\mathrm{m}}.\hat{\mathrm{s}}^{-1}) &= c(\mathrm{m.s^{-1}}) \end{aligned}$$

The redefined system of units is then;

$$\begin{aligned} 1\mathrm{s} &= \omega\hat{\mathrm{s}} \\ 1\mathrm{m} &= \frac{\omega}{c}\hat{\mathrm{m}} = k_0\hat{\mathrm{m}} \\ 1\mathrm{A} &= \sqrt{\frac{\mu_0}{\omega c}}\hat{\mathrm{A}} = \sqrt{\frac{\mu_0}{k_0 c^2}}\hat{\mathrm{A}} \\ 1\mathrm{kg} &= 1\hat{\mathrm{kg}} \\ 1\mathrm{V} &= \frac{1}{c^2}\sqrt{\frac{1}{\mu_0 k_0}}\hat{\mathrm{V}} \\ 1\Omega &= \frac{1}{\mu_0 c}\hat{\Omega} \\ 1\Omega.\mathrm{m} &= \frac{\omega}{\mu_0 c^2}\hat{\Omega}.\hat{\mathrm{m}} = \frac{k_0}{\mu_0 c}\hat{\Omega}.\hat{\mathrm{m}} \\ 1\mathrm{W} &= k_0^2\omega^{-3}\hat{\mathrm{W}} \end{aligned}$$

3 Variational principle for multiple loops

Consider some distribution of currents flowing in some complicated way around the antenna structure, where we for the moment ignore the sources and conductors that are guiding it to flow in that way. These currents will generate an electric field in the region of the (for the moment non existent) antenna. We would like to choose an arrangement of currents so that the electric field at some places is zero, representing the conducting surfaces of the antenna. The sources driving the current are represented by small demons at some places, which force a voltage difference across a small gap. The problem then is to determine this as yet unknown current distribution. This problem is solved by describing an arbitary current distribution in terms of a linear combination of possible distributions and choosing these linear factors with a variational approach. We consider the case of L loops of conducting ribbon, and try to find the self-consistent current distribution which satisfies the following along the middle of each loop;

$$E_l(\xi) = V_l\delta(\xi) + \frac{\rho}{w_l} I_l(\xi) \qquad \text{for } \xi \text{ on } C_l \tag{1}$$

where C_l is the contour around the middle of the l'th loop (of width w_l), we have a slice generator of voltage V_l at $\xi = 0$, ρ is the surface resistivity of the loop, and $I_l(\xi)$ is the current in the loop. It is assumed that the ribbon is thin enough to have a uniform current and voltage distribution across it. This condition may be thought of as saying that the external inductance dominates the internal inductance of the loop. The delta function represents the demon driving the current, the so-called slice-generator.

It is frequently too restrictive to specify only a voltage source at the slice generator, so a slightly more flexible Thevenin equivalent source is used;

$$U_l = I_l(0)X_l + V_l \tag{2}$$

where U_l is the source voltage and X_l the source internal impedance. A fixed current per loop can then be specified by choosing a sufficiently large value for X_l.

Equation 1 is converted into a computationaly useful form using a variational principle, namely that we can express an equation $y(x) = 0$ in a integral form by using;

$$g, y \in \mathcal{T}(\mathcal{S})$$

then

$$\int_S y(x)g(x)dx = 0 \; \forall \, g(x) \;\Leftrightarrow\; y(x) = 0 \; \forall \, x \in S$$

where S is some interval and $\mathcal{T}$ is a closed subspace of $\mathcal{H}(S)$, the space of all functions defined on S. That is we can ensure $y = 0$, by checking that the inner product of a function y with all test functions from some closed subspace is zero. In reality we choose a finite dimensional subspace of $\mathcal{H}(S)$, and increase the dimension until convergence, i.e. until our subspace is sufficiently big to accurately represent the real $y(x)$. Examples of such subspaces include the piecewise continuous functions on a grid, or as is to be used here, a truncated Fourier series. As the dimension of the subspace is increased, by adding more modes, any error in the solution of the equation is restricted to a space disjunct to that represented.

In our case S is the set of contours around the loops,and y corresponds to the equation eq.1. We then represent develop the space $\mathcal{H}$ as a sum of Fourier modes, and the subspace $\mathcal{T}$ is this summation truncated at some Fourier mode. Any error will then have only components at the high Fourier modes not included in the sum, and the low Fourier modes will still be correct. For the currents in the loops we then have;

$$I_l(\xi) = \sum_{p=-P}^{P} I_{pl} e^{ipn_{\xi l}\xi} \tag{3}$$

where $n_{\xi l} = 2\pi/l_l$ and l_l is the length of the contour around the l'th loop. The current supplied by the slice generator is given by

$$I_l(0) = \sum_{p=-P}^{P} I_{pl} \tag{4}$$

The test functions g also come from the truncated Fourier space $\mathcal{T}$ and since any test function in $\mathcal{T}$ can be represented as a linear combination of the basis finctions, it is sufficient to satisfy the equation eq.1 for each of the Fouries modes. Equation eq.1 then becomes a set of $L(2p+1)$ equations, i.e. $(2p+1)$ "test inner products" on each of L contours.

$$V_l = \sum_{p'=-P}^{P} \sum_{l'=1}^{L} I_{p'l'} \left(Z_{pl}^{p'l'} - \delta_{-p,p'} \delta_{-l,l'} R_l \right) \qquad \forall p, l \tag{5}$$

where $R_l = \rho l_l / w_l$ is the total resistance of the l'th loop, and

$$Z_{pl}^{p'l'} = \oint_{C_l} e^{ipn_{\xi l}\xi} E^{p'l'}(\xi)\, d\xi \tag{6}$$

are the partial impedances. $E^{p'l'}$ is the electric field due to a unit current in Fourier mode p' on loop l' i.e. $(I_{pl} = 1)$. Combining equations 2, 4 and 5 a simple set of linear equations is achieved, expressed in a matrix form as:

$$\left(\begin{pmatrix} Z_{-P,1}^{-P,1} & Z_{-P,1}^{-P+1,1} & \cdots & Z_{-P,1}^{P,L} \\ Z_{-P+1,1}^{-P,1} & Z_{-P+1,2}^{-P+1,1} & \cdots & Z_{-P+1,1}^{P,L} \\ \vdots & & & \\ Z_{P,L}^{-P,1} & Z_{P,L}^{-P+1,1} & \cdots & Z_{P,L}^{P,L} \end{pmatrix} + \right. \tag{7}$$

$$\left. \begin{pmatrix} (X_1 - R_1)\mathbf{I} & \cdots & 0 \\ \vdots & \ddots & \cdots \\ 0 & \cdots & (X_L - R_L)\mathbf{I} \end{pmatrix} \right) \begin{pmatrix} I_{11} \\ \vdots \\ I_{PL} \end{pmatrix} = \begin{pmatrix} U_1 \\ \vdots \\ U_1 \\ U_2 \\ \vdots \\ U_2 \\ \vdots \\ U_L \end{pmatrix} \tag{8}$$

By far the greatest effort is in the calculation of the partial impedances $Z_{pl}^{p'l'}$. Once the partial impedance matrix Z has been calculated for a particular configuration, is is very easy to calculate the antenna currents resulting from an arbitary set of driving sources (U_l, X_l)

4 Calculation of $Z_{pl}^{p'l'}$

Unlike conventional engineering antenna problems, where wave propagation is usually into an isotropic, homogeneous, non-dispersive media, for ICRH antennas the plasma presents a surface impedance which is a strong function of both the polarization and the imposed wave numbers in at the surface. Is is conventionally solved in Fourier space in the poloidal (m) and toroidal (n) directions, with the total field being a sum of the independent Fourier modes and the two polarizations of the field. The summations are terminated at some finite m and n, where the contribution to the antenna field is sufficiently small. Consider loops of poloidal width $2\Phi_l$ extending radially from $r = r_1$ to $r = r_2$ and centered on $\phi = \Phi_{l0}$, $z = z_{l0}$.

$$
\begin{aligned}
Z_{pl}^{p'l'} &= \oint E^{p'l'}(\xi)\, e^{ipn_{\xi l}\xi} \cdot d\xi = \sum_n \sum_m \left(\int_1 + \int_2 + \int_3 + \int_4 \right) \\
&= \sum_n \sum_m e^{im\Phi_{l0}} e^{inz_{l0}/R} \Big(- \int_{-\Phi_l}^{\Phi_l} -E_{\phi,mn}^{p'l'}(r_2) e^{im\phi} \cdot e^{i\psi_1} e^{-ipn_{\xi l} r_2 \phi} r_2 d\phi \\
&\qquad - \int_{r_1}^{r_2} -E_{r,mn}^{p'l'}(r) e^{-im\Phi_l} \cdot e^{i\psi_2} e^{-ipn_{\xi l}(r-r_0)} dr \\
&\qquad + \int_{-\Phi_l}^{\Phi_l} +E_{\phi,mn}^{p'l'}(r_1) e^{im\phi} \cdot e^{i\psi_3} e^{ipn_{\xi l} r_1 \phi} r_1 d\phi \\
&\qquad + \int_{r_1}^{r_2} +E_{r,mn}^{p'l'}(r) e^{im\Phi_l} \cdot e^{i\psi_4} e^{ipn_{\xi l}(r-r_0)} dr \Big)
\end{aligned} \tag{9}
$$

Where $E_{mn}^{p'l'}$ is the (m,n) Fourier component of the electric field generated by a unit current in mode p' on loop l'. Note that the contour integral, the current and the phase propagation of the normal modes proceed in the clockwise direction. The ψ correspond to the phase of the normal mode in the middle of each leg and are given by;

$$
\begin{aligned}
\psi_1 &= pn_{\xi 0} d_l \\
\psi_2 &= pn_{\xi 0}(d_l + r_2\Phi + (r_2 - r_0) \\
\psi_3 &= pn_{\xi 0}(d_l + (r_2 + r_1)\Phi + (r_2 - r_1) \\
\psi_4 &= pn_{\xi 0}(d_l + (r_2 + 2r_1)\Phi + (r_0 + r_2 - 2r_1)
\end{aligned}
$$

where d_l is the distance of the slice generator along the strap anticlockwise from $\phi = \Phi_l$, $r = r_2$.

Noting that $\mathrm{sinc}(x) = \sin(x)/x$, equation 9 becomes;

$$
\begin{aligned}
Z_{pl}^{p'l'} &= \sum_m \sum_n e^{im\Phi_{l0}} e^{inz_{l0}/R} \Big[-2r_2\Phi_l E_{\phi,mn}^{p'l'}(r_2) e^{i\psi_1} \mathrm{sinc}((m - pn_{\xi 0} r_2)\Phi) \\
&\quad + 2r_1\Phi_l E_{\phi,mn}^{p'l'}(r_1) e^{i\psi_3} \mathrm{sinc}((m + pn_{\xi 0} r_1)\Phi) \\
&\quad - e^{-im\Phi} e^{i\psi_2} \int_{r_1}^{r_2} E_{r,mn}^{p'l'}(r) e^{-ipn_{\xi 0}(r-r_0)} dr \\
&\quad + e^{im\Phi} e^{i\psi_4} \int_{r_1}^{r_2} E_{r,mn}^{p'l'}(r) e^{ipn_{\xi 0}(r-r_0)} dr \Big]
\end{aligned} \tag{10}
$$

Since the $E_r(r)$ will be given in terms of a local power series about $r = r_0$, we also need;

$$
\int_{x_1}^{x_2} \sum_{k=0}^{n} a_k x^k e^{\nu x} = \sum_{k=0}^{n} a_k \left[\frac{e^{\nu x}}{\nu^{k+1}} k!(-1)^k \sum_{j=0}^{k} \frac{(-\nu x)^j}{j!} \right]_{x_1}^{x_2} \tag{11}
$$

Unfortunately, this analytically correct expression is numerically unusable for large n because the inner sum (over j) tends to $e^{-\nu x}$ so that $e^{\nu x}$ times the sum tends towards unity for both

x_1 and x_2. The integral is then the small difference between these numbers, giving rise to catastrophic cancellation. Accumulating the running difference between the x_1 and x_2 terms does not help, because the two indefinite integrals will tend to unity (with increasing k) at different rates. The solution is to make use of the identity;

$$e^x \sum_{j=0}^{k} \frac{(-x)^j}{j!} = 1 - e^x \sum_{j=k+1}^{\infty} \frac{(-x)^j}{j!} \tag{12}$$

where the infinite sum on the RHS converges quickly and can be terminated when the terms no longer contribute to the sum (in the numerical sense) and the constant 1 can be neglected as it cancels when the upper and lower indefinite integrals are subtracted.

5 Derivation of the wave equations in vacuum

Since the loops comprising the antenna array are near the vessel wall, well away from the plasma, and are usually protected by limiters and a Faraday screen, it suffices to consider the solution of the wave equation in the region between plasma and wall as being a vacuum. In this section we derive the Fourier decomposed wave equations in this vacuum region, including the effects of the current source terms at the current sheets (antenna back and front) and the radial volume current.

5.1 Maxwell's equations in cylindrical geometry with radial current

Taking units where $\mu_0, c, \omega = 1$, Fourier decomposing with respect to time, ϕ (poloidal angle) and z (axial position); i.e. all fields vary as $f(r)e^{i(m\phi+n_z z-\omega t)}$ and setting $n_\phi = \frac{m}{r}$ Maxwell's $\nabla \times \vec{E} = -\frac{\partial \vec{B}}{\partial t}$ equation becomes,

$$in_\phi E_z - in_z E_\phi = iH_r \tag{13}$$

$$in_z E_r - E'_z = iH_\phi \tag{14}$$

$$E'_\phi + \frac{E_\phi}{r} - in_\phi E_r = iH_z \tag{15}$$

and Maxwell's $\nabla \times \vec{B} = \mu_0 \vec{J} + \frac{1}{c^2}\frac{\partial \vec{E}}{\partial t}$ equation becomes,

$$in_\phi H_z - in_z H_\phi = J_r - iE_r \tag{16}$$

$$in_z H_r - H'_z = J_\phi - iE_\phi \tag{17}$$

$$H'_\phi + \frac{H_\phi}{r} - in_\phi H_r = J_z - iE_z \tag{18}$$

Solving for the r and ϕ components of the electromagnetic field in terms of only the source current and the z (axial) components of the fields gives,

$$(14)+(16) \Rightarrow \quad (1-n_z^2)E_r = in_z E'_z - n_\phi H_z - iJ_r \tag{19}$$

$$(17)+(13) \Rightarrow \quad (1-n_z^2)E_\phi = -n_\phi n_z E_z - iH'_z - iJ_\phi \tag{20}$$

$$(17)+(13) \Rightarrow \quad (1-n_z^2)H_r = n_\phi E_z + in_z H'_z + in_z J_\phi \tag{21}$$

$$(14)+(16) \Rightarrow \quad (1-n_z^2)H_\phi = iE'_z - n_\phi n_z H_z - in_z J_r \tag{22}$$

Since the antenna loops to be modelled will be considered having the front and back surface at a constant radii, they will take the form of current sheets, and will appear only as discontinuities in the fields at those radii. The radial feeds however must be explicitly included in the wave equations in the radial region that antenna loops are present.

It will be seen that the Maxwells equations decouple into two second order differential equations, corresponding to two independent wave polarizations.

5.2 Derivation of 2nd order D.E. for $E_z \neq 0$ waves

Using equations 14 and 16 above, eliminating E_r and solving for E'_z gives,

$$\begin{aligned} E'_z &= n_z(J_r - in_\phi H_z + in_z H_\phi) - iH_\phi \\ &= n_z J_r - i(1-n_z^2)H_\phi - in_\phi n_z H_z \end{aligned}$$

taking the derivative w.r.t. r of this and noting that,

$$n'_\phi = \left(\frac{m}{r}\right)' = -\frac{m}{r^2} = -\frac{n_\phi}{r}$$

gives,

$$\begin{aligned}
E_z'' &= n_z J_r' - i(1-n_z^2)H_\phi' - in_\phi n_z H_z' + \frac{i}{r}n_\phi n_z H_z \\
&= n_z J_r' - i(1-n_z^2)\left(-iE_z - \frac{H_\phi}{r} + in_\phi H_r\right) - in_\phi n_z(in_z H_r + iE_\phi) + \frac{i}{r}n_\phi n_z H_z \\
&= n_z J_r' + i(1-n_z^2)\left(iE_z + \frac{H_\phi}{r}\right) + n_\phi(n_\phi E_z - n_z E_\phi) + n_\phi n_z E_\phi + \frac{i}{r}n_\phi n_z H_z \\
&= n_z J_r' - (1-n_z^2)E_z + n_\phi^2 E_z - \frac{1}{r}(-i(1-n_z^2)H_\phi - in_\phi n_z H_z) \\
&= n_z J_r' - (1-n_z^2-n_\phi^2)E_z - \frac{1}{r}(E_z' - n_z J_r)
\end{aligned}$$

Where 18 is used in the 2nd line, 13 is used in the 3rd line and 22 is used in the 5th line. Using $n_\phi = \frac{m}{r}$ and rearranging terms gives the final D.E.,

$$E_z'' + \frac{E_z'}{r} + \left(1 - n_z^2 - \frac{m^2}{r^2}\right)E_z = n_z\left(J_r' + \frac{J_r}{r}\right) \tag{23}$$

where the LHS is a normal 2nd order homogeneous Bessel equation, and the RHS contains information only about the radial current source term.

5.3 Derivation of 2nd order D.E. for $H_z \neq 0$ waves

Using equations 13 and 17 above, eliminating H_r and solving for H_z' gives,

$$\begin{aligned}
H_z' &= in_z(n_\phi E_z - n_z E_\phi) + iE_\phi \\
&= i(1-n_z^2)E_\phi + in_\phi n_z E_z
\end{aligned}$$

taking the derivative w.r.t. r gives,

$$\begin{aligned}
H_z'' &= i(1-n_z^2)E_\phi' + in_\phi n_z E_z' - \frac{i}{r}n_\phi n_z E_z \\
&= i(1-n_z^2)\left(iH_z - \frac{E_\phi}{r} + in_\phi E_r\right) + in_\phi n_z\left(in_z E_r - iH_\phi\right) - \frac{i}{r}n_\phi n_z E_z \\
&= -(1-n_z^2)H_z - \frac{i}{r}(1-n_z^2)E_\phi + in_\phi(J_r - in_\phi H_z + in_z H_\phi) + n_\phi n_z H_\phi - \frac{i}{r}n_\phi n_z E_z \\
&= -(1-n_z^2-n_\phi^2)H_z + in_\phi J_r - \frac{H_z'}{r}
\end{aligned}$$

Using $n_\phi = \frac{m}{r}$ and rearranging terms gives the final D.E.,

$$H_z'' + \frac{H_z'}{r} + \left(1 - n_z^2 - \frac{m^2}{r^2}\right)H_z = i\frac{m}{r}J_r \tag{24}$$

where the LHS is a normal 2nd order homogeneous Bessel equation, and the RHS contains information only about the radial current source term.

6 Fields generated by a loop antenna

In this section we derive the full electromagnetic field of a poloidal loop antenna extending poloidaly 2Φ and radially from $r = r_1$ to $r = r_2$ with strap width $2w$ and centered at $\phi = \Phi_0$, $z = z_0$. We will consider the fields generated by the J_ϕ and J_r current components separately. It should be noted that it is extremely important to correctly calculate the fields generated by the antenna, with particular care to the field matching at the discontinuities, because unlike the antenna calculations using the induced EMF method [8], where one simply calculates the linked magnetic flux by a loop, in this case the fields of the assumed current distribution give rise to surface charge densities on the antenna surface. Although in the total, summed field the fields from these charges are small and give rise to negligible , capacitive loading, the wave fields generated by individual antenna modes may have large surface charge distributions. For example at low frequency those antenna modes with several wavelengths around a loop will generate very large accumlations of charge and high electric fields, however the condition of zero electric field along the loop specifies that the contribution from such modes in the final solution should be very small.

6.1 Fields due to J_ϕ current components

6.1.1 Fourier components

Current flows in the $+\phi$ direction on the plasma facing leg of the loop.

$$J_\phi(\phi,z,r) = \begin{cases} f(z)(+e^{i\psi_3}e^{ipn_{\xi 0}r_1(\phi-\Phi_0)}\delta(r-r_1) - e^{i\psi_1}e^{-ipn_{\xi 0}r_2(\phi-\Phi_0)}\delta(r-r_2)) \\ \qquad\qquad \Phi_0-\Phi<\phi<\Phi_0+\Phi \\ 0 \qquad\qquad \text{otherwise} \end{cases} \tag{25}$$

Fourier decomposing with respect to z and ϕ gives.

$$\begin{aligned} J_\phi(m,n,r) &= +\frac{F(n)}{2\pi}\delta(r-r_1)e^{i\psi_3}\int_{\Phi_0-\Phi}^{\Phi_0+\Phi} e^{-im\phi}e^{i(\phi-\Phi_0)(pn_{\xi 0}r_1)}d\phi \\ &\quad -\frac{F(n)}{2\pi}\delta(r-r_2)e^{i\psi_1}\int_{\Phi_0-\Phi}^{\Phi_0+\Phi} e^{-im\phi}e^{i(\phi-\Phi_0)(-pn_{\xi 0}r_2)}d\phi \\ &= \Phi e^{-im\Phi_0}\frac{F(n)}{\pi}\Big(\delta(r-r_1)e^{i\psi_3}\mathrm{sinc}((pn_{\xi 0}r_1-m)\Phi) \qquad (26) \\ &\quad -\delta(r-r_2)e^{i\psi_1}\mathrm{sinc}((pn_{\xi 0}r_2+m)\Phi)\Big) \qquad (27) \end{aligned}$$

where the integrals are first simplified by the substitution $\theta = \phi - \Phi_0$ we put $\mathrm{sinc}(x) \equiv \sin(x)/x$ and,

$$F(n) = \frac{1}{2\pi R}\int_{-\pi R}^{\pi R} f(z)e^{-inz/R}dz$$

For a current distribution that is uniform across a ribbon of width $2w$ centred at $z = 0$, and carrying a unit total current we have;

$$\begin{aligned} F(n) &= \frac{1}{2\pi R}\int_{z_0-w}^{z_0+w}\frac{1}{2w}e^{-inz/R}dz \\ &= \frac{1}{4\pi Rw}\frac{1}{-in/R}\Big[e^{-inz/R}\Big]_{z_0-w}^{z_0+w} \\ &= e^{-inz_0/r}\frac{i}{4\pi wn}2i\sin(-nw/R) \\ &= \frac{1}{2\pi R}e^{-inz_0/R}\mathrm{sinc}(nw/R) \end{aligned} \tag{28}$$

6.1.2 Full electromagnetic field around a current sheet

Consider a cylindrical current sheet at radius $r = \rho$.

$$J(r,\theta,z,t) = (J_\phi \underline{\hat{\phi}} + J_z \underline{\hat{z}})\delta(r-\rho)e^{i(m\theta+nz/R-\omega t)}$$

The problem is to determine the full electromagnetic field associated with this sheet. Since we have previously seen that Maxwell's equations in vacuum in cylindrical geometry reduce to second order Bessel equations in E_z and H_z, without any loss of generality we can assume the solutions are of the form,

$$E_z = \begin{cases} AI_m(hr) & \text{when } r < \rho \\ BK_m(hr) & \text{when } r > \rho \end{cases}$$

$$H_z = \begin{cases} CI_m(hr) & \text{when } r < \rho \\ DK_m(hr) & \text{when } r > \rho \end{cases}$$

where $h = \sqrt{|1-n_z^2|}$ and $I_m \to J_m$ and $K_m \to H_m^{(1)}$ when $n_z < 1$ (due to causality, only the outwardly propagating Hankel function is reasonable). Since E_z is radially continuous, we have;

$$AI_m(h\rho) = BK_m(h\rho)$$

Noting that H_r, E_z and E_ϕ are radially continuous, and that J_ϕ is zero immediately on either side of the current sheet, we can see from the ϕ component of Maxwell's curl H equation that H_z' is the same on both sides of the current sheet, i.e.

$$CI_m'(h\rho) = DK_m'(h\rho)$$

and that there is a discontinuity in H_z due to the J_ϕ current sheet given by,

$$\Delta H_z = H_z(\rho^+) - H_z(\rho^-) = -J_\phi$$

i.e.

$$DK_m(h\rho) - CI_m(h\rho) = -J_\phi$$

The z component of Maxwell's curl H equation, together with the radial continuity of H_r and E_z shows that H_ϕ is discontinuous and finite due to the J_z current sheet, with the discontinuity given by,

$$\Delta H_\phi = J_z$$

Eliminating E_r between $[\nabla \times E = iH]_\phi$ and $[\nabla \times H = -iE]_r$ gives

$$(1-n_z^2)H_\phi = iE_z' - \frac{m}{r}n_z H_z$$

Since we already know that H_z and H_ϕ are discontinuous at $r = \rho$ we deduce that E_z' is also discontinuous, with the discontinuity given by,

$$\Delta E_z' = -i(1-n_z^2)\Delta H_\phi - i\frac{m}{r}n_z \Delta H_z$$

i.e.

$$BK_m'(h\rho) - AI_m'(h\rho) = -\frac{i}{h}(1-n_z^2)J_z + \frac{im}{hr}n_z J_\phi$$

This set of 4 equations has the solutions,

$$A = \frac{iK_m(h\rho)}{h\mathcal{W}}\left((1-n_z^2)J_z - \frac{m}{\rho}n_z J_\phi\right)$$

$$C = -\frac{K'_m(h\rho)}{\mathcal{W}} J_\phi$$

where $\mathcal{W} = (K_m I'_m - I_m K'_m)(h\rho)$ is the Wronskian. The other field components are given by,

$$\begin{aligned} E_\phi &= -\frac{mn_z}{rn_\perp^2} E_z - \frac{i}{n_\perp^2} H'_z \\ &= -\frac{i\varepsilon\rho n_z m}{rh} J_z K_m(h\rho) I_m(hr) + \frac{i\varepsilon m^2 n_z^2}{rhn_\perp^2} J_\phi K_m(h\rho) I_m(hr) \\ &\quad + \frac{hi\varepsilon\rho}{n_\perp^2} J_\phi K'_m(h\rho) I'_m(hr) \end{aligned}$$

$$\begin{aligned} H_\phi &= \frac{i}{n_\perp^2} E'_z - \frac{mn_z}{rn_\perp^2} H_z \\ &= -\varepsilon\rho K_m(h\rho) I'_m(hr) J_z + \frac{\varepsilon m n_z}{n_\perp^2} J_\phi K_m(h\rho) I'_m(hr) \\ &\quad + \frac{mn_z\varepsilon\rho}{rn_\perp^2} J_\phi K'_m(h\rho) I_m(hr) \\ &= -\varepsilon\rho K_m(h\rho) I'_m(hr) J_z + \frac{\varepsilon m n_z}{n_\perp^2} J_\phi \left(K_m(h\rho) I'_m(hr) + \frac{\rho}{r} K'_m h\rho I_m(hr) \right) \end{aligned}$$

For the case $\rho > r$ we define the following matrix operators.

$$A_\rho(r) = \varepsilon \begin{pmatrix} \frac{i\rho n_\perp^2}{h} K_m(h\rho) I_m(hr) & , & -\frac{imn_z}{h} K_m(h\rho) I_m(hr) \\ -\frac{imn_z\rho}{rh} K_m(h\rho) I_m(hr) & , & \frac{ih\rho}{n_\perp^2} K'_m(h\rho) I'_m(hr) + \frac{im^2 n_z^2}{rhn_\perp^2} K_m(h\rho) I_m(hr) \end{pmatrix} \tag{29}$$

$$B_\rho(r) = \varepsilon \begin{pmatrix} 0 & , & -\rho K'_m(h\rho) I_m(hr) \\ -\rho K_m(h\rho) I'_m(hr) & , & \frac{mn_z\rho}{rn_\perp^2} K'_m(h\rho) I_m(hr) + \frac{mn_z}{n_\perp^2} K_m(h\rho) I'_m(hr) \end{pmatrix} \tag{30}$$

When $\rho < r$ I_m is replaced by K_m and K_m by I_m. The total perpendicular field at radius r due to current sheets at $r = \rho_i$, $J(r) = \delta(r - \rho_i)(\hat{z} J_z^{(i)} + \hat{\phi} J_\phi^{(i)})$ is then;

$$\Theta(r) \equiv \begin{pmatrix} E_z(r) \\ E_\phi(r) \\ H_z(r) \\ H_\phi(r) \end{pmatrix} = \sum_i \begin{pmatrix} A_{\rho_i}(r) \\ B_{\rho_i}(r) \end{pmatrix} \begin{pmatrix} J_z^{(i)} \\ J_\phi^{(i)} \end{pmatrix} \tag{31}$$

6.1.3 Calculation of the Wronskian

Reference [15] gives;

$$\mathcal{W}(K_m, I_m) = \frac{1}{r}$$

So in our case;

$$\mathcal{W}(K_m(hr), I_m(hr))(hr) = \frac{1}{hr}$$

Where it is very important to note that the derivative in the Wronskian is simply with respect to the argument i.e. hr, since the $\frac{d}{dr}(hr) = h$ is already counted.

When we have $n_z < 1$ i.e. propagating waves we want,

$$\begin{aligned} \mathcal{W}(H_m^1(z), J_m(z))(z) &= H_m^1 J'_m - J_m H_m^{1\prime} \\ &= (J_m + iY_m) J'_m - J_m (J'_m + iY'_m) \\ &= iY_m J'_m - iJ_m Y'_m \\ &= i\mathcal{W}(Y_m, J_m) \\ &= -i\mathcal{W}(J_m, Y_m) \\ &= -\frac{2i}{\pi z} \qquad \text{A \& S} \end{aligned}$$

In the previously mentioned generalized Bessel notation we have;

$$\mathcal{W}(K_m, I_m)(hr) = \frac{1}{\varepsilon r}$$

where we define.

$$\varepsilon = \begin{cases} h & n_z > 1 \\ i\pi h/2 & n_z < 1 \end{cases}$$

6.2 Fields due to J_r current components

The second order DEs for the electromagnetic field due to the radial currents will naturally have a homogeneous part, corresponding to the solution of the source free equations, and a particular solution, with the radial volume sources included. Although is is possible to get an analytical expression for the particular solution (see appendix), this expression must be numerically computed (it contains an infinite power series). It was considered simpler to solve for the particular solution directly as a power series, since it can then also be easily integrated as required later for the calculation of the partial impedances.

6.2.1 Matching fields from J_r volume currents

We want to have the total electromagnetic field due to a radial volume current with a particular poloidal and toroidal fourier mode. The solution is simply to solve the two independent 2nd order wave equations (E_z and H_z) subject to the source terms. It is important to note that the continuity and boundary conditions are given by the differential equation itself and not "imposed" from some additional knowledge. Also note that the volume charge and the charge sheet arising from the discontinuity in J_r are automatically incorporated in this solution.

E_z waves

We have;

$$E_z = \begin{cases} E_i I_m(hr) & \text{when } r < r_1 \\ E_1 I_m(hr) + E_2 K_m(hr) + \mathcal{E}(r) & \text{when } r_1 < r < r_2 \\ E_o K_m(hr) & \text{when } r > r_2 \end{cases} \tag{32}$$

Where $\mathcal{E}$ is a solution to the inhomogeneous wave equation, i.e. with the radial current source terms. Continuity of E_z at r_1 and r_2 gives;

$$\begin{aligned} E_i I_m(hr_1) &= E_1 I_m(hr_1) + E_2 K_m(hr_1) + \mathcal{E}(r_1) \\ E_o K_m(hr_2) &= E_1 I_m(hr_2) + E_2 K_m(hr_2) + \mathcal{E}(r_2) \end{aligned}$$

Inspection of the differential equation for E_z shows that as we approach the limit where the radial discontinuity in J_r is infinitely steep, only the E_z and J_r' terms are significant. Considering a discontinuity at $r = \rho$ we have in the vicinity of $r = \rho$

$$J_r' \approx \delta(r - \rho)(J_r(\rho^-) - J_r(\rho^+))$$

and

$$E_z'' \approx n_z J_r' \text{ at } r = r_1 \text{ and } r = r_2$$

giving

$$(E_z')' = n_z \delta(r - \rho)(J_r(\rho^-) - J_r(\rho^+))$$

so that E_z' is discontinuous,

$$E_z'(\rho^+) - E_z'(\rho^-) = n_z(J_r(\rho^-) - J_r(\rho^+))$$

i.e. $E_z' - n_z J_r$ is continuous. Imposing this condition at r_1 and r_2 gives;

$$\begin{aligned} E_i h I_m'(hr_1) &= E_1 h I_m'(hr_1) + E_2 h K_m'(hr_1) + \mathcal{E}'(r_1) - n_z J_r(r_1) \\ E_o h K_m'(hr_2) &= E_1 h I_m'(hr_2) + E_2 h K_m'(hr_2) + \mathcal{E}'(r_2) - n_z J_r(r_2) \end{aligned}$$

Dividing the two equations for $r = r_1$ we get,

$$\frac{I_m(hr_1)}{hI_m'(hr_1)} = \frac{E_1 I_m(hr_1) + E_2 K_m(hr_1) + \mathcal{E}(r_1)}{E_1 h I_m'(hr_1) + E_2 h K_m'(hr_1) + \mathcal{E}'(r_1) - n_z J_r(r_1)}$$

$$E_1 h I_m I_m' + E_2 h K_m' I_m + \mathcal{E}' I_m - n_z J_r I_m = E_1 h I_m' I_m + E_2 h K_m I_m' + h\mathcal{E} I_m'$$

$$E_2(hK_m' I_m - hI_m' K_m) = hI_m' \mathcal{E} - I_m \mathcal{E}' + n_z J_r I_m$$

$$E_2 = \frac{hI_m'(hr_1)\mathcal{E}(r_1) - I_m(hr_1)\mathcal{E}'(r_1) + n_z J_r(r_1) I_m(hr_1)}{hK_m'(hr_1) I_m(hr_1) - hI_m'(hr_1) K_m(hr_1)} \tag{33}$$

Dividing the two equations for $r = r_2$ we get,

$$\frac{K_m(hr_2)}{hK_m'(hr_2)} = \frac{E_1 I_m(hr_2) + E_2 K_m(hr_2) + \mathcal{E}(r_2)}{E_1 h I_m'(hr_2) + E_2 h K_m'(hr_2) + \mathcal{E}'(r_2) - n_z J_r(r_2)}$$

$$E_1 h I_m' K_m + E_2 h K_m' K_m + \mathcal{E}' K_m - n_z J_r K_m = E_1 h I_m K_m' + E_2 h K_m K_m' + h\mathcal{E} K_m'$$

$$E_1(hI_m' K_m - hK_m' I_m) = hK_m' \mathcal{E} - K_m \mathcal{E}' + n_z J_r K_m$$

$$E_1 = \frac{hK_m'(hr_2)\mathcal{E}(r_2) - K_m(hr_2)\mathcal{E}'(r_2) + n_z J_r(r_2) K_m(hr_2)}{hI_m'(hr_2) K_m(hr_2) - hK_m'(hr_2) I_m(hr_2)} \tag{34}$$

Substituting back into the continuity equations for E_z we get,

$$E_i = E_1 + E_2 \frac{K_m(hr_1)}{I_m(hr_1)} + \frac{\mathcal{E}(r_1)}{I_m(hr_1)} \tag{35}$$

$$E_o = E_1 \frac{I_m(hr_2)}{K_m(hr_2)} + E_2 + \frac{\mathcal{E}(r_2)}{K_m(hr_2)} \tag{36}$$

H_z waves

The continuity requirements at r_1 and r_2 are that H_z and E_ϕ be continuous. This gives formula the same as for E_z but with no J_r term.

6.2.2 Fourier components and power series representation

Current flows radially inwards at $\phi = \Phi_0 - \Phi$ and radially outward at $\phi = \Phi_0 + \Phi$.

$$J_r(\phi, z, r) = \begin{cases} f(z)\Big(+ \delta(r(\phi - \Phi_0 - \Phi)) e^{i\psi_4 + ipn\xi_0(r-r_0)} - \delta(r(\phi - \Phi_0 + \Phi)) e^{i\psi_2 - ipn\xi_0(r-r_0)} \Big) & \\ \qquad\qquad r_1 < r < r_2 & \\ 0 \qquad\qquad \text{otherwise} & \end{cases}$$

Fourier decomposing in the z and ϕ directions gives;

$$J_r(m, n, r) = \frac{F(n)}{2\pi r} e^{-im\Phi_0} \Big(+ e^{-im\Phi} e^{i\psi_4} e^{ipn\xi_0(r-r_0)} - e^{im\Phi} e^{i\psi_2} e^{-ipn\xi_0(r-r_0)} \Big) \tag{37}$$

To get power series for the terms in r we proceed;

$$\frac{1}{r} e^{\nu(r-r_0)} = \frac{1}{r} \sum_{k=0}^{\infty} \frac{\nu^k (r - r_0)^k}{k!} = \sum_{k=0}^{\infty} a_k (r - r_0)^k$$

where

$$\nu = ipn_{\xi 0}$$

Multiplying the last two equalities through by $r = r_0 + (r - r_0)$.

$$\sum_{k=0}^{\infty} \frac{\nu^k (r-r_0)^k}{k!} = \sum_{k=0}^{\infty} r_0 a_k (r-r_0)^k + \sum_{k=1}^{\infty} a_{k-1}(r-r_0)^k$$

The constant term is;

$$1 = r_0 a_0$$

$$a_0 = 1/r_0 \tag{38}$$

The term in $(r - r_0)^k$, for $k \geq 1$ is;

$$\frac{\nu^k}{k!} = r_0 a_k + a_{k-1}$$

$$a_k = \frac{1}{r_0}\left(\frac{\nu^k}{k!} - a_{k-1}\right) \tag{39}$$

giving

$$J_r(m,n,r) = \begin{cases} \frac{F(n)}{2\pi} e^{-im\Phi_0} \left[e^{-im\Phi} e^{i\psi_4} \sum_{k=0}^{\infty} a_k (r-r_0)^k - e^{im\Phi} e^{i\psi_2} \sum_{k=0}^{\infty} a_k^{\star} (r-r_0)^k \right] \\ \qquad\qquad \text{when } r_1 < r < r_2 \\ 0 \qquad\qquad \text{otherwise} \end{cases} \tag{40}$$

Useful also is;

$$\begin{aligned} J_r' + \frac{J_r}{r} &= \frac{ipn_{\xi 0} F(n)}{2\pi r} e^{-im\Phi_0} \left(e^{-im\Phi} e^{i\psi_4} e^{ipn_{\xi 0}(r-r_0)} + e^{im\Phi} e^{i\psi_2} e^{-ipn_{\xi 0}(r-r_0)} \right) \\ &= \frac{ipn_{\xi 0} F(n)}{2\pi} e^{-im\Phi_0} \left[e^{-im\Phi} e^{i\psi_4} \sum_{k=0}^{\infty} a_k (r-r_0)^k + e^{im\Phi} e^{i\psi_2} \sum_{k=0}^{\infty} a_k^{\star} (r-r_0)^k \right] \end{aligned}$$

6.2.3 Particular solution for H_z waves

Consider the 2nd order D.E. with an inhomogeneous term e^{ar}/r^2.

$$y'' + \frac{y'}{r} + \left(1 - n^2 - \frac{m^2}{r^2}\right) y = C \frac{e^{\nu(r-r_0)}}{r^2} \tag{41}$$

Expanding y and the inhomogeneous term in power series;

$$y = \sum_{k=0}^{\infty} a_k (r-r_0)^k \tag{42}$$

$$e^{\nu(r-r_0)^k} = \sum_{k=0}^{\infty} \frac{\nu^k (r-r_0)^k}{k!}$$

we get;

$$\begin{aligned} 0 &= \sum_{k=2}^{\infty} a_k k(k-1)(r-r_0)^{k-2} + \sum_{k=1}^{\infty} a_k k \frac{1}{r} (r-r_0)^{k-1} \\ &\quad + \sum_{k=1}^{\infty} a_k \left(1 - n^2 - \frac{m^2}{r^2}\right)(r-r_0)^k - \sum_{k=0}^{\infty} \frac{C}{r^2} \frac{\nu^k (r-r_0)^k}{k!} \end{aligned}$$

multiplying throught by r^2 and changing variable to $x = r - r_0$ gives;

$$\begin{aligned} 0 &= \sum_{k=2}^{\infty} a_k k(k-1)(x+r_0)^2 x^{k-2} + \sum_{k=1}^{\infty} a_k k(x+r_0)x^{k-1} \\ &\quad + \sum_{k=1}^{\infty}((1-n^2)(x+r_0)^2 - m^2)a_k x^k - \sum_{k=0}^{\infty} C\frac{\nu^k x^k}{k!} \end{aligned}$$

expanding the above;

$$\begin{aligned} 0 &= \sum_{k=2}^{\infty} a_k k(k-1)\left[x^k + 2r_0 x^{k-1} + r_0^2 x^{k-2}\right] + \sum_{k=1}^{\infty} a_k k\left[x^k + r_0 x^{k-1}\right] \\ &\quad + \sum_{k=0}^{\infty} a_k\left[(1-n^2)x^{k-2} + 2r_0(1-n^2)x^{k+1} + (r_0^2(1-n^2) - m^2)x^k\right] - \sum_{k=0}^{\infty} C\frac{\nu^k}{k!}x^k \end{aligned}$$

which contains only terms in x^k where $k \geq 0$. For the initial conditions at $r = r_0$ we have;

$$a_0 = y(r_0) \tag{43}$$

$$a_1 = y'(r_0) \tag{44}$$

From the x^0 term we get an equation for a_2 ;

$$2a_2 r_0^2 + a_1 r_0 + a_0(r_0^2(1-n^2) - m^2) - C = 0 \tag{45}$$

From the x^1 term we get an equation for a_3 ;

$$4a_2 r_0 + 6a_3 r_0^2 + a_1 + 2a_2 r_0 + 2a_0 r_0(1-n^2) + a_1(r_0^2(1-n^2) - m^2) - C\nu = 0 \tag{46}$$

The other a_k follow from the x_k terms. For $k \geq 2$ we have ;

$$\begin{aligned} 0 &= a_k k(k-1) + 2r_0 a_{k+1}(k+1)k + r_0^2 a_{k+2}(k+2)(k+1) + ka_k + r_0 a_{k+1}(k+1) \\ &\quad + (1-n^2)a_{k-2} + 2r_0(1-n^2)a_{k-1} + (r_0^2(1-n^2) - m^2)a_k - C\frac{\nu^k}{k!} \end{aligned}$$

Collecting terms;

$$\begin{aligned} 0 &= a_{k-2}\left[1-n^2\right] + a_{k-1}\left[2r_0(1-n^2)\right] + a_k\left[k(k-1) + k + (r_0^2(1-n^2) - m^2)\right] \\ &\quad + a_{k+1}\left[2r_0 k(k+1) + r_0(k+1)\right] + a_{k+2}\left[r_0^2(k+2)(k+1)\right] - C\frac{\nu^k}{k!} \end{aligned}$$

Simplifying;

$$\begin{aligned} 0 &= a_{k-2}\left[1-n^2\right] + a_{k-1}\left[2r_0(1-n^2)\right] + a_k\left[k^2 - m^2 + r_0^2(1-n^2)\right] \\ &\quad + a_{k+1}\left[r_0(k+1)(2k+1)\right] + a_{k+2}\left[r_0^2(k+2)(k+1)\right] - C\frac{\nu^k}{k!} \end{aligned}$$

Shifting k down by 2 gives a_k for $k \geq 4$;

$$\begin{aligned} a_k\left[r_0^2 k(k-1)\right] &= C\frac{\nu^{k-2}}{(k-2)!} - (1-n^2)\left[a_{k-4} + 2r_0 a_{k-3} + r_0^2 a_{k-2}\right] \\ &\quad - a_{k-2}\left[(k-2)^2 - m^2\right] - a_{k-1} r_0\left[(k-1)(2k-3)\right] \end{aligned} \tag{47}$$

6.2.4 Particular solution of E_z waves

Consider the 2nd order D.E. with the inhomogeneous term e^{ar}/r.

$$y'' + \frac{y'}{r} + \left(1 - n^2 - \frac{m^2}{r^2}\right) y = C\frac{e^{\nu(r-r_0)}}{r} \tag{48}$$

Expanding y and the inhomogeneous term in power series;

$$y = \sum_{k=0}^{\infty} a_k (r - r_0)^k \tag{49}$$

$$e^{\nu(r-r_0)^k} = \sum_{k=0}^{\infty} \frac{\nu^k (r - r_0)^k}{k!}$$

we get;

$$\begin{aligned} 0 &= \sum_{k=2}^{\infty} a_k k(k-1)(r-r_0)^{k-2} + \sum_{k=1}^{\infty} a_k k \frac{1}{r}(r-r_0)^{k-1} \\ &\quad + \sum_{k=1}^{\infty} a_k \left(1 - n^2 - \frac{m^2}{r^2}\right)(r-r_0)^k - \sum_{k=0}^{\infty} \frac{C}{r}\frac{\nu^k (r-r_0)^k}{k!} \end{aligned}$$

multiplying throught by r^2 and changing variable to $x = r - r_0$ gives;

$$\begin{aligned} 0 &= \sum_{k=2}^{\infty} a_k k(k-1)(x+r_0)^2 x^{k-2} + \sum_{k=1}^{\infty} a_k k(x+r_0)x^{k-1} \\ &\quad + \sum_{k=1}^{\infty} ((1-n^2)(x+r_0)^2 - m^2) a_k x^k - \sum_{k=0}^{\infty} C(x+r_0)\frac{\nu^k x^k}{k!} \end{aligned}$$

expanding the above;

$$\begin{aligned} 0 &= \sum_{k=2}^{\infty} a_k k(k-1)\left[x^k + 2r_0 x^{k-1} + r_0^2 x^{k-2}\right] + \sum_{k=1}^{\infty} a_k k\left[x^k + r_0 x^{k-1}\right] \\ &\quad + \sum_{k=0}^{\infty} a_k \left[(1-n^2)x^{k-2} + 2r_0(1-n^2)x^{k+1} + (r_0^2(1-n^2) - m^2)x^k\right] - \sum_{k=0}^{\infty} C\frac{\nu^k}{k!}\left[(x^{k+1} + r_0 x^k\right] \end{aligned}$$

which contains only terms in x^k where $k \geq 0$. For the initial conditions at $r = r_0$ we have;

$$a_0 = y(r_0) \tag{50}$$

$$a_1 = y'(r_0) \tag{51}$$

From the x^0 term we get an equation for a_2 ;

$$2a_2 r_0^2 + a_1 r_0 + a_0(r_0^2(1-n^2) - m^2) - Cr_0 = 0 \tag{52}$$

From the x^1 term we get an equation for a_3 ;

$$4a_2 r_0 + 6a_3 r_0^2 + a_1 + 2a_2 r_0 + 2a_0 r_0(1-n^2) + a_1(r_0^2(1-n^2) - m^2) - C(1 + \nu r_0) = 0 \tag{53}$$

The other a_k follow from the x_k terms. For $k \geq 2$ we have ;

$$\begin{aligned} 0 &= a_k k(k-1) + 2r_0 a_{k+1}(k+1)k + r_0^2 a_{k+2}(k+2)(k+1) + k a_k + r_0 a_{k+1}(k+1) \\ &\quad + (1-n^2)a_{k-2} + 2r_0(1-n^2)a_{k-1} + (r_0^2(1-n^2) - m^2)a_k - C\frac{\nu^{k-1}}{(k-1)!} - Cr_0\frac{\nu^k}{k!} \end{aligned}$$

Collecting terms;

$$0 = a_{k-2}\left[1-n^2\right] + a_{k-1}\left[2r_0(1-n^2)\right] + a_k\left[k(k-1)+k+(r_0^2(1-n^2)-m^2)\right]$$
$$+a_{k+1}\left[2r_0k(k+1)+r_0(k+1)\right] + a_{k+2}\left[r_0^2(k+2)(k+1)\right] - C\frac{\nu^{k-1}}{(k-1)!}\left(1+\frac{\nu}{k}r_0\right)$$

Simplifying;

$$0 = a_{k-2}\left[1-n^2\right] + a_{k-1}\left[2r_0(1-n^2)\right] + a_k\left[k^2-m^2+r_0^2(1-n^2)\right]$$
$$+a_{k+1}\left[r_0(k+1)(2k+1)\right] + a_{k+2}\left[r_0^2(k+2)(k+1)\right] - C\frac{\nu^{k-1}}{(k-1)!}\left(1+\frac{\nu}{k}r_0\right)$$

Shifting k down by 2 gives a_k for $k \geq 4$;

$$a_k\left[r_0^2k(k-1)\right] = C\frac{\nu^{k-3}}{(k-3)!}\left(1+\frac{\nu}{(k-2)}r_0\right) - (1-n^2)\left[a_{k-4}+2r_0a_{k-3}+r_0^2a_{k-2}\right]$$
$$-a_{k-2}\left[(k-2)^2-m^2\right] - a_{k-1}r_0\left[(k-1)(2k-3)\right] \tag{54}$$

6.2.5 Divide local power series by r

Since it will be necessary to know H_z/r later, and the solution is in the form of a power series, we need to know how to divide the power series by r. Putting

$$\frac{1}{r}\sum_{k=0}^{\infty} b_k(r-r_0)^k = \sum_{k=0}^{\infty} a_k(r-r_0)^k$$

Multiply through by $r = r_0 + (r-r_0)$

$$\sum_{k=0}^{\infty} b_k(r-r_0)^k = \sum_{k=0}^{\infty} r_0a_k(r-r_0)^k + \sum_{k=1}^{\infty} a_{k-1}(r-r_0)^k$$

The $k=0$ term gives;

$$b_0 = r_0a_0$$

That is;

$$a_0 = b_0/r_0 \tag{55}$$

And the $k \geq 1$ terms give;

$$b_k = r_0a_k + a_{k-1}$$

That is;

$$a_k = \frac{1}{r_0}(b_k - a_{k-1}) \tag{56}$$

7 Matrix formulation of the boundary equations

The image currents that flow in the three current sheets representing (a) the vessel wall (b) the antenna's Faraday screen and (c) the plasma surface are calculated from the imposed antenna current distribution by imposing the apropriate boundary conditions relating the electric field in the surface with the induced current. The 6 equations that determine the 6 unknown currents $\underline{J}$ flowing in the 3 current sheets may be formulated;

$$\underline{\underline{M}}(\underline{\Phi}^J + \underline{\Phi}^A) - \underline{\underline{\eta}}\underline{J} = \underline{0} \tag{57}$$

with the solution,

$$\underline{J} = (\underline{\underline{\eta}} - \underline{\underline{M}}\,\underline{\underline{N}})^{-1}\underline{\underline{M}}\,\underline{\Phi}^A \tag{58}$$

Where we define;

$$\underline{\underline{\eta}} = \begin{pmatrix} \eta_w & 0 & \cdot & \cdot & \cdot & \cdot \\ 0 & \eta_w & \cdot & \cdot & \cdot & \cdot \\ \cdot & \cdot & & & \cdot & \cdot \\ \cdot & \cdot & & \underline{\underline{\eta}}^{(f)} & \cdot & \cdot \\ \cdot & \cdot & \cdot & \cdot & 0 & 0 \\ \cdot & \cdot & \cdot & \cdot & 0 & 0 \end{pmatrix} \tag{59}$$

And where $\underline{\underline{\eta}}^{(f)}$ is the surface impedance of the Faraday screen, noting that (i) shield angle and (ii) a perpendicular admittance (capacitance between rods) and (iii) a parallel admittance (rod inductance) are possible in this formulation. The boundary equations themselves appear in $\underline{\underline{M}}$ as;

$$\underline{\underline{M}} = \begin{pmatrix} 1 & \cdot & \cdot & \cdot & \cdot & \cdot \\ \cdot & 1 & \cdot & \cdot & \cdot & \cdot \\ \cdot & \cdot & 1 & \cdot & \cdot & \cdot \\ \cdot & \cdot & \cdot & 1 & \cdot & \cdot \\ \cdot & \cdot & \cdot & \cdot & 1 & \cdot \\ \cdot & \cdot & \cdot & \cdot & \cdot & -\underline{\underline{\eta}}_p \end{pmatrix} \tag{60}$$

The vector $\underline{\Phi}$ contains the perpendicular field components at the current sheets, and the superscript ^{J} or ^{A} refers to whether those fields are from the current sheets or the antenna field, respectively. The former defines $\underline{\underline{N}}$;

$$\underline{\Phi}^J = \begin{pmatrix} A_w(w) & , & A_f(w) & , & A_p(w) \\ A_w(f) & , & A_f(f) & , & A_p(f) \\ A_w(p) & , & A_f(p) & , & A_p(p) \\ B_w(p) & , & B_f(p) & , & B_p(p) \end{pmatrix} \begin{pmatrix} J_z^{(w)} \\ J_\phi^{(w)} \\ J_z^{(f)} \\ J_\phi^{(f)} \\ J_z^{(p)} \\ J_\phi^{(p)} \end{pmatrix} = \underline{\underline{N}}\,\underline{J} \tag{61}$$

And $\underline{\Phi}^A$ is determined by solving the Maxwell's equations for the antenna structure currents in the absence of the current sheets.

$$\underline{\Phi} = \left(E_z^A(w), E_\phi^A(w), E_z^A(f), E_\phi^A(f), E_z^A(p), E_\phi^A(p), H_z^A(p), H_\phi^A(p)\right)^T \tag{62}$$

8 Faraday screen

The Faraday screen is modelled as a sheet of anisotropic conductivity located at a fixed radius. Assuming a coordinate system in which the anisotropy in the conductivity is resolved into parallel and perpendicular components, where $\hat{\mathbf{e}}_{\|}$ is an angle ϕ rotated from the axial direction $\hat{\mathbf{z}}$ in the $\hat{\phi}$ direction, i.e.

$$\begin{pmatrix} E_z \\ E_\phi \end{pmatrix} = R \begin{pmatrix} E_{\|} \\ E_\perp \end{pmatrix} = \begin{pmatrix} \cos\phi & -\sin\phi \\ \sin\phi & \cos\phi \end{pmatrix} \begin{pmatrix} E_{\|} \\ E_\perp \end{pmatrix}$$

in this rotated frame we have,

$$\begin{pmatrix} E_{\|} \\ E_\perp \end{pmatrix} = \begin{pmatrix} \eta_{\|} & 0 \\ 0 & \eta_\perp \end{pmatrix} \begin{pmatrix} J_{\|} \\ J_\perp \end{pmatrix}$$

converting back to $\phi - z$ coordinates we get,

$$\begin{pmatrix} E_z \\ E_\phi \end{pmatrix} = R \begin{pmatrix} \eta_{\|} & 0 \\ 0 & \eta_\perp \end{pmatrix} R^{-1} \begin{pmatrix} J_z \\ J_\phi \end{pmatrix} = \underline{\underline{\eta}} \begin{pmatrix} J_z \\ J_\phi \end{pmatrix}$$

where

$$\begin{aligned} \underline{\underline{\eta}} &= \begin{pmatrix} \cos\phi & -\sin\phi \\ \sin\phi & \cos\phi \end{pmatrix} \begin{pmatrix} \eta_{\|} & 0 \\ 0 & \eta_\perp \end{pmatrix} \begin{pmatrix} \cos\phi & \sin\phi \\ -\sin\phi & \cos\phi \end{pmatrix} \\ &= \begin{pmatrix} \cos\phi & -\sin\phi \\ \sin\phi & \cos\phi \end{pmatrix} \begin{pmatrix} \eta_{\|}\cos\phi & \eta_{\|}\sin\phi \\ -\eta_\perp\sin\phi & \eta_\perp\cos\phi \end{pmatrix} \\ &= \begin{pmatrix} \eta_{\|}\cos^2\phi + \eta_\perp\sin^2\phi & (\eta_{\|} - \eta_\perp)\sin\phi\cos\phi \\ (\eta_{\|} - \eta_\perp)\sin\phi\cos\phi & \eta_{\|}\sin^2\phi + \eta_\perp\cos^2\phi \end{pmatrix} \end{aligned}$$

This formulation should be general enough to incorporate the following:

1. The anisotropic conductivity of the Faraday screen.
2. The Rod to Rod Capacitive current (negligible at low freq).

$$\eta_\perp = \frac{j}{\pi\varepsilon_0 d\omega}\cosh^{-1}\frac{d}{2a} \quad \Omega/\text{square} \tag{63}$$

where d is the rod separation and a is the rod radius

3. Simulate decrease in the axial magnetic field due to the Faraday screen by specifying an effective inductive component to the perpendicular conductivity, thus allowing surface currents in the Faraday screen to screen out some of the magnetic field.

9 Surface impedance without plasma

Since the fields decay rapidly from the antenna surface for very high poloidal and toroidal mode numbers, the antenna does not "see" the plasma, and so it is reasonable to ignore the presence of the plasma and just consider the surface impedance in its absence. This "vaccum" surface impedance matrix is also quickly computed and is useful for testing the code.

9.1 $H_z \neq 0$, $H_\phi = 0$ waves

$$\begin{aligned} H_z &= I_m(hr) \\ H_z' &= hI_m'(hr) \\ E_z &= AI_m(hr) \\ E_z' &= AhI_m'(hr) \end{aligned}$$

Using

$$iE_z' = \frac{m}{r} n_z H_z$$

We can get a value for the constant A in the E_z field.

$$\begin{aligned} ihAI_m'(hr) &= \frac{m}{r} n_z I_m(hr) \\ A &= -\frac{im}{r}\frac{n_z}{h}\frac{I_m(hr)}{I_m'(hr)} \end{aligned}$$

For the E_ϕ field we have;

$$\begin{aligned} E_\phi &= \frac{1}{1-n_z^2}\left(-\frac{m}{r} n_z E_z - iH_z'\right) \\ &= \frac{1}{n_\perp^2}\left(-\frac{m}{r} n_z \left(-\frac{im}{r}\frac{n_z}{h}\frac{I_m(hr)^2}{I_m'(hr)}\right) - ihI_m'(hr)\right) \end{aligned}$$

This gives the surface impedance coefficients;

$$\eta_{fs} \equiv \frac{E_z}{H_z} = -\frac{imn_z}{hr}\frac{I_m(hr)}{I_m'(hr)} \tag{64}$$

$$\eta_{ff} \equiv \frac{E_\phi}{H_z} = \frac{i}{n_\perp^2}\left(-h\frac{I_m'(hr)}{I_m(hr)} + \frac{m^2 n_z^2}{hr^2}\frac{I_m(hr)}{I_m'(hr)}\right) \tag{65}$$

9.2 $H_\phi \neq 0$, $H_z = H_z' = 0$ waves

$$\begin{aligned} H_z &= 0 \\ H_z' &= 0 \\ E_z &= I_m(hr) \\ E_z' &= hI_m'(hr) \end{aligned}$$

For the other fields we have.

$$H_\phi = \frac{1}{1-n_z^2} iE_z' = \frac{ih}{n_\perp^2} I_m'(hr)$$

$$E_\phi = \frac{1}{1-n_z^2}\left(-\frac{m}{r} n_z E_z\right) = -\frac{mn_z}{rn_\perp^2} I_m(hr)$$

This gives the surface impedance coefficients;

$$\eta_{ss} \equiv -\frac{E_z}{H_\phi} = +\frac{in_\perp^2}{h}\frac{I_m(hr)}{I_m'(hr)} \tag{66}$$

$$\eta_{sf} \equiv -\frac{E_\phi}{H_\phi} = -i\frac{mn_z}{rh}\frac{I_m(hr)}{I_m'(hr)} \tag{67}$$

9.3 Tensor form for η_p

$$\begin{pmatrix} E_z \\ E_\phi \end{pmatrix} = \underline{\underline{\eta}}_p \begin{pmatrix} H_z \\ H_\phi \end{pmatrix} \tag{68}$$

Following the convention of Puri (Phys. Fluids 27(8) Aug 1984) for the plasma surface impedance tensor terms we have.

$$\underline{\underline{\eta}}_p = \begin{pmatrix} \eta_{fs} & -\eta_{ss} \\ \eta_{ff} & -\eta_{sf} \end{pmatrix} \tag{69}$$

10 Calculation of the plasma surface impedance matrix

In this section the wave equations will be integrated in the radial direction by framing them in a variational form and then numerically solving this variational form using cubic-hermite finite elements. The cold plasma wave equations have solutions with perpendicular wavelengths that vary by several orders of magnitude, the fast wave and the slow wave. The fast wave typically has perpendicular wavelengths of the same order as the plasma radius and gradients, and must therefore be numerically integrated usually with some higher order shooting method. The slow wave has a very short perpendicular wavelength and so can be solved in a simple WKB approach, however when one requires both, a numerical problem occurs in that shooting methods fail due to the growth of the slow mode, which although in principle is suppressed by the boundary conditions, eventually dominates the fast wave solution and gives rise to a numerically unstable system. Global solution methods such as finite differences and finite element methods implicitly apply the boundary conditions at both sides of the interval and so the unwanted contribution from the fast growing solution is no longer a numerical problem.

10.1 The dielectric tensor

As we have chosen cylindrical geometry, the only heating scenario that can be modelled is the Alfvén wave case. It suffices for this case to use the cold plasma dielectric tensor with first order thermal corrections [14]. This allows modelling of the mode conversion of the fast wave to the slow wave, and Landau damping at the Alfvén resonance layer.

$$\epsilon = \begin{pmatrix} \epsilon_\xi & -i\epsilon_\eta & 0 \\ i\epsilon_\eta & \epsilon_\xi & 0 \\ 0 & 0 & \epsilon_\zeta \end{pmatrix}$$

where

$$\begin{aligned} \epsilon_\xi &= 1 - \sum_j \frac{\omega_{pj}^2}{1-\omega_{cj}^2} \\ \epsilon_\eta &= \sum_j \frac{\omega_{cj}\omega_{pj}^2}{1-\omega_{cj}^2} \\ \epsilon_\zeta &= 1 - \sum_j \zeta_j^2 Z'(\zeta_j^2) \frac{\omega_{pj}^2}{1-\omega_{cj}^2} \end{aligned}$$

and

$$\begin{aligned} \omega_{pj}^2 &= \frac{n_j q_j^2}{m_j \varepsilon_0} \\ \omega_{cj} &= \frac{q_j B}{m_j} \\ \zeta_j &= \frac{c}{k_\parallel v_{th,j}} \end{aligned}$$

Z is the plasma dispersion function, $Z'(\zeta) = -2(1+\zeta Z(\zeta))$, $v_{th,j}$ is the thermal speed, m_j the mass, q_j the charge and n_j the number density of the j'th species.

Since we will frame the wave equations in terms of the magnetic field components, it is more useful to have the plasma magnetization tensor.

$$\kappa = \epsilon^{-1} = \begin{pmatrix} \kappa_\xi & i\kappa_\eta & 0 \\ -i\kappa_\eta & \kappa_\xi & 0 \\ 0 & 0 & \kappa_\zeta \end{pmatrix}$$

$$\begin{aligned}
\epsilon_\perp^2 &= \epsilon_\xi^2 - \epsilon_\eta^2 \\
\kappa_\xi &= \frac{\epsilon_\xi}{\epsilon_\perp^2} \\
\kappa_\eta &= \frac{\epsilon_\eta}{\epsilon_\perp^2} \\
\kappa_\zeta &= \frac{1}{\epsilon_\zeta}
\end{aligned}$$

10.2 Local coordinate system

The flux surfaces in the plasma are assumed to be circular and concentric with a rotational transform $q(r)$ giving a the local equilibrium magnetic field an angle χ to the axial direction.

$$\begin{aligned}
(r,\theta,z) &\rightarrow (\xi,\eta,\zeta) \\
\hat{\zeta} &= S\hat{\theta} + C\hat{z} \\
\hat{\eta} &= C\hat{\theta} - S\hat{z} \\
\hat{z} &= -S\hat{\eta} + C\hat{\zeta} \\
\hat{\theta} &= C\hat{\eta} + S\hat{\zeta}
\end{aligned}$$

where

$$\begin{aligned}
S &= \sin(\chi) \\
C &= \cos(\chi) \\
\tan\chi &= \frac{B_\phi}{B_0} = \frac{r}{qr_T} \\
\chi' &= CS(\frac{1}{r} - \frac{q'}{q}) \\
\chi'_m &= \chi' - \frac{CS}{r} \\
\chi'_p &= \chi' + \frac{CS}{r}
\end{aligned}$$

10.3 Useful vector identities in (ξ,η,ζ) coordinates

$$\nabla\times(A_\mu\hat{\mu}) = A_\mu\nabla\times\hat{\mu} - \hat{\mu}\times\nabla A_\mu$$

$$\begin{aligned}
\nabla\times\hat{r} &= 0 \\
\nabla\times\hat{\theta} &= \frac{\hat{z}}{r} \\
\nabla\times\hat{z} &= 0
\end{aligned}$$

$$\begin{aligned}
\nabla\phi &= \frac{\partial\phi}{\partial r}\hat{\xi} + in_\eta\phi\hat{\eta} + in_\zeta\phi\hat{\zeta} \\
\nabla\cdot\mathbf{A} &= \frac{1}{r}\frac{\partial}{\partial r}(rA_\xi) + in_\eta A_\eta + in_\zeta A_\zeta
\end{aligned}$$

$$\nabla\times\hat{\xi} = 0$$

$$\nabla \times \hat{\eta} = C\nabla \times \hat{\theta} - \hat{\theta} \times \nabla C + \hat{z} \times \nabla S = \frac{C^2}{r}\hat{\zeta} + \chi'_m \hat{\eta}$$

$$\nabla \times \hat{\zeta} = -\hat{z} \times \nabla C + S\nabla \times \hat{\theta} - \hat{\theta} \times \nabla S = \chi'_p \hat{\zeta} - \frac{S^2}{r}\hat{\eta}$$

$$\nabla \times \mathbf{A} = -\hat{r} \times \left[\frac{\partial A_r}{\partial \eta}\hat{\eta} + \frac{\partial A_r}{\partial \zeta}\hat{\zeta}\right] + A_\eta \left[\frac{C^2}{r}\hat{\zeta} + \chi'_m \hat{\eta}\right]$$

$$-\hat{\eta} \times \left[\frac{\partial A_\eta}{\partial r}\hat{r} + \frac{\partial A_\eta}{\partial \zeta}\hat{\zeta}\right] + A_\zeta \left[\chi'_p \hat{\zeta} - \frac{S^2}{r}\hat{\eta}\right] - \hat{\zeta} \times \left[\frac{\partial A_\zeta}{\partial r}\hat{r} + \frac{\partial A_\zeta}{\partial \eta}\hat{\eta}\right]$$

$$= -in_\eta A_r \hat{\zeta} + in_\zeta A_r \hat{\eta} + \frac{C^2}{r}A_\eta \hat{\zeta} + \chi'_m A_\eta \hat{\eta} + A'_\eta \hat{\zeta}$$

$$-in_\zeta A_\eta \hat{r} + \chi'_p A_\zeta \hat{\zeta} - \frac{S^2}{r}A_\zeta \hat{\eta} - A'_\zeta \hat{\eta} + in_\eta A_\zeta \hat{r}$$

$$\begin{aligned}
(\nabla \times \mathbf{A})_\xi &= -in_\zeta A_\eta + in_\eta A_\zeta \\
(\nabla \times \mathbf{A})_\eta &= in_\zeta A_\xi + \chi'_m A_\eta - \frac{S^2}{r}A_\zeta - A'_\zeta \\
(\nabla \times \mathbf{A})_\zeta &= -in_\eta A_\xi + \frac{C^2}{r}A_\eta + A'_\eta + \chi'_p A_\zeta
\end{aligned}$$

$$\begin{aligned}
(\nabla \times \mathbf{A}^*)_\xi &= in_\zeta A^*_\eta - in_\eta A^*_\zeta \\
(\nabla \times \mathbf{A}^*)_\eta &= -in_\zeta A^*_\xi + \chi'_m A^*_\eta - \frac{S^2}{r}A^*_\zeta - A^{*\prime}_\zeta \\
(\nabla \times \mathbf{A}^*)_\zeta &= in_\eta A^*_\xi + \frac{C^2}{r}A^*_\eta + A^{*\prime}_\eta + \chi'_p A^*_\zeta
\end{aligned}$$

$$\begin{aligned}
(\kappa \cdot \nabla \times \mathbf{H})_\xi &= -n_\zeta \kappa_\eta H_\xi + i(-n_\zeta \kappa_\xi + \chi'_m \kappa_\eta)H_\eta + i(n_\eta \kappa_\xi - \frac{S^2}{r}\kappa_\eta)H_\zeta - i\kappa_\eta H'_\zeta \\
(\kappa \cdot \nabla \times \mathbf{H})_\eta &= in_\zeta \kappa_\xi H_\xi + (\chi'_m \kappa_\xi - n_\zeta \kappa_\eta)H_\eta + (n_\eta \kappa_\eta - \frac{S^2}{r}\kappa_\xi)H_\zeta - \kappa_\xi H'_\zeta \\
(\kappa \cdot \nabla \times \mathbf{H})_\zeta &= \kappa_\zeta(-in_\eta H_\xi + \frac{C^2}{r}H_\eta + H'_\eta + \chi'_p H_\zeta)
\end{aligned}$$

$$\begin{aligned}
\nabla \times \hat{\xi}\tilde{H}^*_\xi &= -in_\zeta \tilde{H}^*_\xi \hat{\eta} + in_\eta \tilde{H}^*_\xi \hat{\zeta} \\
\nabla \times \hat{\eta}\tilde{H}^*_\eta &= in_\zeta \tilde{H}^*_\eta \hat{\xi} + \chi'_m \tilde{H}^*_\eta \hat{\eta} + (\frac{C^2}{r}\tilde{H}^*_\eta + \tilde{H}^{*\prime}_\eta)\hat{\zeta} \\
\nabla \times \hat{\zeta}\tilde{H}^*_\zeta &= -in_\eta \tilde{H}^*_\zeta \hat{\xi} - (\frac{S^2}{r}\tilde{H}^*_\zeta + \tilde{H}^{*\prime}_\zeta)\hat{\eta} + \chi'_p \tilde{H}^*_\zeta \hat{\zeta}
\end{aligned}$$

$$\mathbf{H} \cdot \tilde{\mathbf{H}}^* = H_\xi \tilde{H}^*_\xi + H_\eta \tilde{H}^*_\eta + H_\zeta \tilde{H}^*_\zeta$$

10.4 Maxwells equations

The Maxwell's equations in the previously defined dimensionless units may be written as;

$$\begin{aligned}
\nabla \times \mathbf{E} &= i\mathbf{H} \\
\nabla \times \mathbf{H} &= -i\epsilon \cdot \mathbf{E} + \mathbf{J}
\end{aligned}$$

where $\mathbf{J}$ represents all the externally imposed current sources such as the antenna and ϵ contains all the information about the plasma. Since the plasma wave solutions are known to have singular behaviour in the electric field at the Alfvén resonance, the wave equations will be formulated in terms of the wave magnetic field, which has a much smoother behaviour. A variational representation of the wave equation is formed by taking the dot product of Maxwell's curl H equation with a "test" vector field $\nabla \times \tilde{\mathbf{H}}^*$, and integrating over the solution domain. This particular choice of test function allows, after some vector manipulation, an expression involving a volume integral of only first derivatives of the fields, which will mean that in principle the functions used to represent the fields need only be continuous.

$$
\begin{aligned}
\mathbf{E} &= i(\kappa \cdot \nabla \times \mathbf{H} - k \cdot \mathbf{J}) \\
\mathbf{E} \cdot (\nabla \times \tilde{\mathbf{H}}^*) &= i\left[(\kappa \cdot \nabla \times \mathbf{H}) \cdot (\nabla \times \tilde{\mathbf{H}}^*) - (\kappa \cdot \mathbf{J}) \cdot (\nabla \times \tilde{\mathbf{H}}^*)\right] \\
\nabla \cdot (\mathbf{E} \times \tilde{\mathbf{H}}^*) &= (\nabla \times \mathbf{E}) \cdot \tilde{\mathbf{H}}^* - \mathbf{E} \cdot (\nabla \times \tilde{\mathbf{H}}^*) = i\mathbf{H} \cdot \tilde{\mathbf{H}}^* - \mathbf{E} \cdot (\nabla \times \tilde{\mathbf{H}}^*) \\
\nabla \cdot (\mathbf{E} \times \tilde{\mathbf{H}}^*) &= i\left[\mathbf{H} \cdot \tilde{\mathbf{H}}^* - (\kappa \cdot \nabla \times \mathbf{H}) \cdot (\nabla \times \tilde{\mathbf{H}}^*) + (\kappa \cdot \mathbf{J}) \cdot (\nabla \times \tilde{\mathbf{H}}^*)\right] \\
-i \int_S (\mathbf{E} \times \tilde{\mathbf{H}}^*) \cdot dS &= \int_V \left[\mathbf{H} \cdot \tilde{\mathbf{H}}^* - (\kappa \cdot \nabla \times \mathbf{H}) \cdot (\nabla \times \tilde{\mathbf{H}}^*) + (\kappa \cdot \mathbf{J}) \cdot (\nabla \times \tilde{\mathbf{H}}^*)\right] dV \quad (70)
\end{aligned}
$$

This equation (70) is the variational form of the wave equation that will be used in the numerical calculations. The surface integral term contains information about the boundary conditions. Since the equation must hold for all test functions $\tilde{\mathbf{H}}^*$ it must also be true for each component of $\tilde{\mathbf{H}}^*$ individually. We will therefore break it down into separate vector compontents.

10.4.1 H_ξ test field

$$RHS = \mathbf{H}\cdot\hat{\xi}\tilde{H}_\xi^* - (\kappa\cdot\nabla\times\mathbf{H})\cdot(\nabla\times\hat{\xi}\tilde{H}_\xi^*)$$

$$\begin{aligned}
&= H_\xi\tilde{H}_\xi^* + in_z\left[in_\zeta\kappa_\xi H_\xi + (\chi'_m\kappa_\xi - n_\zeta\kappa_n)H_\eta + (n_\eta\kappa_\eta - \frac{S^2}{r}\kappa_\xi)H_\zeta - \kappa_\xi H'_\zeta\right]\\
&\quad -in_\eta\left[\kappa_\zeta(-in_\eta H_\xi + \frac{C^2}{r}H_\eta + H'_\eta + \chi'_p H_\zeta)\right]\\
&= \Big[(1 - n_\zeta^2\kappa_\xi - n_\eta^2\kappa_\zeta)H_\xi + i(\chi'_m n_\zeta\kappa_\xi - n_\zeta^2\kappa_\eta - \frac{C^2}{r}n_\eta\kappa_\zeta)H_\eta\\
&\quad -in_\eta\kappa_\zeta H'_\eta + i(-\frac{S^2}{r}n_\zeta\kappa_\xi + n_\eta n_\zeta\kappa_\eta - \chi'_p n_\eta\kappa_\zeta)H_\zeta - in_\zeta\kappa_\xi H'_\zeta\Big]\tilde{H}_\xi^*
\end{aligned}$$

$$\begin{aligned}
&= (a_\xi\tilde{H}_\xi^* + a'_\xi\tilde{H}_\xi^{*\prime})H_\xi + (a_{\xi p}\tilde{H}_\xi^* + a'_{\xi p}\tilde{H}_\xi^{*\prime})H'_\xi\\
&\quad +(b_\xi\tilde{H}_\xi^* + b'_\xi\tilde{H}_\xi^{*\prime})H_\eta + (b_{\xi p}\tilde{H}_\xi^* + b'_{\xi p}\tilde{H}_\xi^{*\prime})H'_\eta\\
&\quad +(c_\xi\tilde{H}_\xi^* + c'_\xi\tilde{H}_\xi^{*\prime})H_\zeta + (c_{\xi p}\tilde{H}_\xi^* + c'_{\xi p}\tilde{H}_\xi^{*\prime})H'_\zeta
\end{aligned}$$

$$a_\xi = 1 - n_\zeta^2\kappa_\xi - n_\eta^2\kappa_\zeta$$

$$a'_\xi = 0, \qquad a_{\xi p} = 0, \qquad a'_{\xi p} = 0$$

$$b_\xi = i(\chi'_m n_\zeta\kappa_\xi - n_\zeta^2\kappa_\eta - \frac{C^2}{r}n_\eta\kappa_\zeta)$$

$$b'_\xi = 0, \qquad b_{\xi p} = -in_\eta\kappa_\zeta, \qquad b'_{\xi p} = 0$$

$$c_\xi = i(-\frac{S^2}{r}n_\zeta\kappa_\xi + n_\eta n_\zeta\kappa_\eta - \chi'_p n_\eta\kappa_\zeta)$$

$$c'_\xi = 0, \qquad c_{\xi p} = -in_\zeta\kappa_\xi, \qquad c'_{\xi p} = 0$$

10.4.2 H_η test field

$$RHS = \mathbf{H}\cdot\hat{\eta}\tilde{H}^*_\eta - (\kappa\cdot\nabla\times H)\cdot(\nabla\times\hat{\eta}\tilde{H}^*_\eta)$$

$$\begin{aligned}
&= H_\eta\tilde{H}^*_\eta + -in_\zeta\left[-n_\zeta\kappa_\eta H_\xi + i(-n_\zeta\kappa_x + \chi'_m\kappa_\eta)H_\eta + i(n_\eta\kappa_\xi - \frac{S^2}{r}\kappa_\eta)H_\zeta - i\kappa_\eta H'_\zeta\right]\tilde{H}^*_\eta \\
&\quad -\chi'_m\left[in_\zeta\kappa_\xi H_\xi + (\chi'_m\kappa_\xi - n_\zeta\kappa_\eta)H_\eta + (n_\eta\kappa_\eta - \frac{S^2}{r}\kappa_\xi)H_\zeta - \kappa_\xi H'_\zeta\right]\tilde{H}^*_\eta \\
&\quad -\left[\kappa_\zeta(-in_\eta H_\xi + \frac{C^2}{r}H_\eta + H'_\eta + \chi'_p H_\zeta)\right](\frac{C^2}{r}\tilde{H}^*_\eta + \tilde{H}^{*\prime}_\eta) \\
&= \left[i(-\chi'_m n_\zeta\kappa_\xi + n_\zeta^2\kappa_\eta + \frac{C^2}{r}n_\eta\kappa_\zeta)\tilde{H}^*_\eta + in_\eta\kappa_\zeta\tilde{H}^{*\prime}_\eta\right]H_\xi \\
&\quad +\left[(1 - n_\zeta^2\kappa_\xi - {\chi'_m}^2\kappa_\xi + 2\chi'_m n_\zeta\kappa_\eta - \frac{C^4}{r^2}\kappa_\zeta)\tilde{H}^*_\eta - \frac{C^2}{r}\kappa_\zeta\tilde{H}^{*\prime}_\eta\right]H_\eta \\
&\quad -\left[\frac{C^2}{r}\tilde{H}^*_\eta + \tilde{H}^{*\prime}_\eta\right]\kappa_\zeta H'_\eta \\
&\quad +\left[(n_\eta n_\zeta\kappa_\xi + \frac{S^2}{r}\chi'_m\kappa_\xi - \frac{S^2}{r}n_\zeta\kappa_\eta - \chi'_m n_\eta\kappa_\eta - \frac{C^2}{r}\chi'_p\kappa_\zeta)\tilde{H}^*_\eta - \chi'_p\kappa_\zeta\tilde{H}^{*\prime}_\eta\right]H_\zeta \\
&\quad -[n_\zeta\kappa_\eta - \chi'_m kx]\,\tilde{H}^*_\eta H'_\zeta
\end{aligned}$$

$$\begin{aligned}
&= (a_\eta\ Fn + a'_\eta\tilde{H}^{*\prime}_\eta)H_\xi + (a_{\eta p}\tilde{H}^*_\eta + a'_{\eta p}\tilde{H}^{*\prime}_\eta)H'_\xi \\
&\quad +(b_\eta\tilde{H}^*_\eta + b'_\eta\tilde{H}^{*\prime}_\eta)H_\eta + (b_{\eta p}\tilde{H}^*_\eta + b'_{\eta p}\tilde{H}^{*\prime}_\eta)H'_\eta \\
&\quad +(c_\eta\tilde{H}^*_\eta + c'_\eta\tilde{H}^{*\prime}_\eta)H_\zeta + (c_{\eta p}\tilde{H}^*_\eta + c'_{\eta p}\tilde{H}^{*\prime}_\eta)H'_\zeta
\end{aligned}$$

$$a_\eta = i(-\chi'_m n_\zeta\kappa_\xi + n_\zeta^2\kappa_\eta + \frac{C^2}{r}n_\eta\kappa_\zeta)$$

$$a'_\eta = in_\eta\kappa_\zeta, \qquad a_{\eta p} = 0, \qquad a'_{\eta p} = 0$$

$$b_\eta = 1 - (n_\zeta^2 + {\chi'_m}^2)\kappa_\xi + 2\chi'_m n_\zeta\kappa_\eta - \left(\frac{C^2}{r}\right)^2\kappa_\zeta$$

$$b'_\eta = -\frac{C^2}{r}\kappa_\zeta, \qquad b_{\eta p} = -\frac{C^2}{r}\kappa_\zeta, \qquad b'_{\eta p} = -\kappa_\zeta$$

$$c_\eta = (n_\eta n_\zeta + \chi'_m\frac{S^2}{r})\kappa_\xi - (\frac{S^2}{r}n_\zeta + \chi'_m n_\eta)\kappa_\eta - \frac{C^2}{r}\chi'_p\kappa_\zeta)$$

$$c'_\eta = -\chi'_p\kappa_\zeta, \qquad c_{\eta p} = \chi'_m\kappa_\xi - n_\zeta\kappa_\eta, \qquad c'_\eta = 0$$

10.4.3 H_ζ test field

$$RHS = \mathbf{H}\cdot\hat{\zeta}\tilde{H}_\zeta^* - (\kappa\cdot\nabla\times\mathbf{H})\cdot(\nabla\times\hat{\zeta}\tilde{H}_\zeta^*)$$

$$\begin{aligned}
&= H_\zeta\tilde{H}_\zeta^* + in_n\left[-n_\zeta\kappa_\eta H_\xi + i(-n_\zeta\kappa_x + \chi_m'\kappa_\eta)H_\eta + i(n_\eta\kappa_\xi - \frac{S^2}{r}\kappa_\eta)H_\zeta - i\kappa_\eta H_\zeta'\right]\tilde{H}_\zeta^* \\
&\quad + \left[in_\zeta\kappa_\xi H_\xi + (\chi_m'\kappa_\xi - n_\zeta\kappa_\eta)H_\eta + (n_\eta\kappa_\eta - \frac{S^2}{r}\kappa_\xi)H_\zeta - \kappa_\xi H_\zeta'\right](\frac{S^2}{r}\tilde{H}_\zeta^* + \tilde{H}_\zeta^{*\prime}) \\
&\quad -\chi_p'\left[\kappa_\zeta(-in_\eta H_\xi + \frac{C^2}{r}H_\eta + H_\eta' + \chi_p' H_\zeta)\right]\tilde{H}_\zeta^* \\
&= \left[i(-n_\eta n_\zeta\kappa_\eta + \frac{S^2}{r}n_\zeta\kappa_\xi + \chi_p' n_\eta\kappa_\zeta)\tilde{H}_\zeta^* + in_\zeta\kappa_\xi\tilde{H}_\zeta^{*\prime}\right]H_\xi \\
&\quad + \left[(n_\eta n_\zeta\kappa_\xi + \frac{S^2}{r}\chi_m'\kappa_\xi - \chi_m' n_\eta\kappa_\eta - \frac{S^2}{r}n_\zeta\kappa_\eta - \frac{C^2}{r}\chi_p'\kappa_\zeta)\tilde{H}_\zeta^* + (\chi_m'\kappa_\xi - n_\zeta\kappa_\eta)\tilde{H}_\zeta^{*\prime}\right]H_\eta \\
&\quad - \left[\chi_p'\kappa_\zeta\tilde{H}_\zeta^*\right]H_\eta' + \left[(1 - n_\eta^2\kappa_\xi - \frac{S^4}{r^2}\kappa_\xi + 2\frac{S^2}{r}n_\eta\kappa_\eta - \chi_p'^2\kappa_\zeta)\tilde{H}_\zeta^* + (n_\eta\kappa_\eta - \frac{S^2}{r}\kappa_\xi)\tilde{H}_\zeta^{*\prime}\right]H_\zeta \\
&\quad + \left[(n_\eta\kappa_\eta - \frac{S^2}{r}\kappa_\xi)\tilde{H}_\zeta^* - \kappa_\xi\tilde{H}_\zeta^{*\prime}\right]H_\zeta'
\end{aligned} \tag{71}$$

$$\begin{aligned}
&= (a_\zeta\tilde{H}_\zeta^* + a_\zeta'\tilde{H}_\zeta^{*\prime})H_\xi + (a_{\zeta p}\tilde{H}_\zeta^* + a_{\zeta p}'\tilde{H}_\zeta^{*\prime})H_\xi' \\
&\quad +(b_\zeta\tilde{H}_\zeta^* + b_\zeta'\tilde{H}_\zeta^{*\prime})H_\eta + (b_{\zeta p}\tilde{H}_\zeta^* + b_{\zeta p}'\tilde{H}_\zeta^{*\prime})H_\eta' \\
&\quad +(c_\zeta\tilde{H}_\zeta^* + c_\zeta'\tilde{H}_\zeta^{*\prime})H_\zeta + (c_{\zeta p}\tilde{H}_\zeta^* + c_{\zeta p}'\tilde{H}_\zeta^{*\prime})H_\zeta'
\end{aligned}$$

$$a_\zeta = i(\frac{S^2}{r}n_\zeta\kappa_\xi - n_\eta n_\zeta\kappa_\eta + \chi_p' n_\eta\kappa_\zeta)$$

$$a_\zeta' = in_\zeta\kappa_\xi, \qquad a_{\zeta p} = 0, \qquad a_{\zeta p}' = 0$$

$$b_\zeta = (n_\eta n_\zeta + \frac{S^2}{r}\chi_m')\kappa_\xi - (\chi_m' n_\eta + \frac{S^2}{r}n_\zeta)\kappa_\eta - \frac{C^2}{r}\chi_p'\kappa_\zeta$$

$$b_\zeta' = \chi_m'\kappa_\xi - n_\zeta\kappa_\eta, \qquad b_{\zeta p} = -\chi_p'\kappa_\zeta, \qquad b_{\zeta p}' = 0$$

$$c_\zeta = 1 - (n_\eta^2 + \frac{S^4}{r^2})\kappa_\xi + 2\frac{S^2}{r}n_\eta\kappa_\eta - \chi_p'^2\kappa_\zeta$$

$$c_\zeta' = n_\eta\kappa_\eta - \frac{S^2}{r}\kappa_\xi, \qquad c_{\zeta p} = n_\eta\kappa_\eta - \frac{S^2}{r}\kappa_\xi, \qquad c_\zeta' = -\kappa_\xi$$

10.5 Cubic hermite representation

The H fields are represented by cubic-hermite finite elements, these have the advantage that the field and its derivative are continuous. Two unknowns per grid point (for each field component) must be specified, the contribution from the two basis functions. For a uniform grid of nodes x_k these are;

$$\psi_k(x) = 1 - 3(x - x_k)^2 + 2(x - x_k)^3 \quad (72)$$

$$\phi_k(x) = (x - x_k) - 2(x - x_k)^2 + (x - x_k)^3 \quad (73)$$

10.6 Integration

The variational form of the wave equations are integrated for each basis function of the test field $(\hat{\mathbf{H}})$ numerically using Gaussion integration over 4 points within each interval $(x_k, x_{k+1}$. This gives rise to a banded matrix linking all fields of adjacent nodes. Since $\nabla \cdot \mathbf{H} = 0$ is an additional condition, which has not yet been used, it can be applied to eliminate H'_ξ and reduce the number of unknowns per node from 6 to 5.

$$H'_\xi = -\left(\frac{1}{r}H_\xi + in_\eta H_\eta + in_\zeta H_\zeta\right)$$

The surface integral term at the origin is included by imposing the analytic approximation near $r = 0$ on the fields at the first node. The surface integral term at the plasma surface is included by using the boundary conditions (a) $(E_\eta, E_\zeta) = (1, 0)$ and (b) $(E_\eta, E_\zeta) = (0, 1)$. The problem is solved for each of these conditions to get $\mathbf{H}$ solutions for each polarization, and hence the full surface impedance matrix.

10.7 Regularity conditions at the origin

The variational form of the wave equation eq.70 requires knowledge of the boundary conditions at the origin and at the plasma surface. The condition at the origin is obtained by examining the form of the wave equations and expressing the field components as a power series in r. The highest order terms in equation are kept and the determinant of the matrix of equations gives the value of the unknown power of r. One solution must be discarded on the grounds that it is ill behaved. The eigenvectors of the matrix represent the two allowed waves, and can be combined to give a resultant surface impedance matrix at a radius near the origin. This radius must be sufficiently small in order to maintain the ordering of terms in the wave equations is maintained. From Puri (Nuc. Fus. Vol.27. No.7 (1987) pp1094) we have;

$$
\begin{aligned}
E'_\eta &= -\left(\frac{C}{r}+\frac{n_\eta\epsilon_\eta}{\epsilon_\xi}\right)E_\eta - \chi'_p E_\zeta + i\frac{n_\eta n_\zeta}{\epsilon_\xi}H_\eta + i\left(1-\frac{n_\eta^2}{\epsilon_\xi}\right)H_\zeta \\
E'_\zeta &= \left(\chi'_m - \frac{n_\zeta\epsilon_\eta}{\epsilon_\xi}\right)E_\eta - \frac{S}{r}E_\zeta - i\frac{\gamma_1}{\epsilon_\xi}H_\eta - i\frac{n_\eta n_\zeta}{\epsilon_\xi}H_\zeta \\
H'_\eta &= -in_\eta n_\zeta E_\eta + i\left(n_\eta^2-\epsilon_\zeta\right)E_\zeta - \frac{C}{r}H_\eta - \chi'_p H_\zeta \\
H'_\zeta &= i\left(\gamma_1 - \frac{\epsilon_\eta^2}{\epsilon_\xi}\right)E_\eta + in_\eta n_\zeta E_\zeta + \left(\chi'_m - \frac{n_\zeta\epsilon_\eta}{\epsilon_\xi}\right)H_\eta + \left(\frac{n_\eta\epsilon_\eta}{\epsilon_\xi}-\frac{S}{r}\right)H_\zeta
\end{aligned}
$$

where

$$
\gamma_1 = \epsilon_\xi - n_\zeta^2 \qquad n_\eta = \frac{m}{r}
$$

$$
\begin{aligned}
\tan\chi &= \frac{r}{qR} \\
S \equiv \sin\chi &= \frac{r}{\sqrt{r^2+q^2R^2}} \\
C \equiv \cos\chi &= \frac{qR}{\sqrt{r^2+q^2R^2}} \\
\frac{CS}{r} &= \frac{qR}{r^2+q^2R^2} \\
\chi' &= \left(\frac{1}{qR}-\frac{rq'}{q^2R}\right)\frac{q^2R^2}{r^2+q^2R^2} \\
\chi'_m \equiv \chi' - \frac{CS}{r} &= -\frac{rRq'}{r^2+q^2R^2} \\
\chi'_p \equiv \chi' + \frac{CS}{r} &= \frac{2qR}{r^2+q^2R^2} - \frac{rRq'}{r^2+q^2R^2}
\end{aligned}
$$

near to r=0 we have;

$$
\begin{aligned}
\frac{S}{r} &\approx \frac{1}{qR} \\
\frac{C}{r} &\approx \frac{1}{r} \\
\chi'_m &\approx -\frac{rq'}{q^2R} \\
\chi'_p &\approx \frac{2}{qR}
\end{aligned}
$$

So we have the ordering of the terms in the wave equations as;

$$\begin{pmatrix} E_\eta \\ E_\zeta \\ H_\eta \\ H_\zeta \end{pmatrix}' \propto \begin{pmatrix} \frac{1}{r} & 1 & \frac{1}{r} & \frac{1}{r^2} \\ 1 & 1 & 1 & \frac{1}{r} \\ \frac{1}{r} & \frac{1}{r^2} & \frac{1}{r} & 1 \\ 1 & \frac{1}{r} & 1 & \frac{1}{r} \end{pmatrix} \begin{pmatrix} E_\eta \\ E_\zeta \\ H_\eta \\ H_\zeta \end{pmatrix}$$

which suggests using;

$$\begin{pmatrix} E_\eta \\ E_\zeta \\ H_\eta \\ H_\zeta \end{pmatrix} = \begin{pmatrix} A \\ Br \\ C \\ Dr \end{pmatrix} r^{\beta-1}$$

The wave equations then become;

$$\begin{pmatrix} (\beta-1)A \\ \beta B \\ (\beta-1)C \\ \beta D \end{pmatrix} = \begin{pmatrix} -\left(1+\frac{m\epsilon_\eta}{\epsilon_\xi}\right) & -\frac{2}{qR}r^2 & +i\frac{mn_\zeta}{\epsilon_\xi} & i\left(r^2-\frac{m^2}{\epsilon_\xi}\right) \\ \left(-\frac{rq'}{q^2R}-\frac{-n_\zeta\epsilon_\eta}{\epsilon_\xi}\right) & \frac{r}{qR} & -i\frac{\gamma_1}{\epsilon_\xi} & -i\frac{mn_\zeta}{\epsilon_\xi} \\ -imn_\zeta & i(m^2-\epsilon_\zeta r^2) & -1 & -\frac{2r^2}{qR} \\ i\left(\gamma_1-\frac{\epsilon_\eta^2}{\epsilon_\xi}\right) & imn_\zeta & -\left(\frac{rq'}{q^2R}+\frac{n_\zeta\epsilon_\eta}{\epsilon_\xi}\right) & \left(\frac{m\epsilon_\eta}{\epsilon_\xi}-\frac{r}{qR}\right) \end{pmatrix} \begin{pmatrix} A \\ B \\ C \\ D \end{pmatrix}$$

The determinant of this set of four equations is $(m^2-\beta^2)^2$, so we only have solutions for $\beta = |m|$, as the $-|m|$ solution diverges at the origin (corresponding to the Y_m or K_m solution to the 2nd order DE. The corresponding eigenvectors are

$$\begin{pmatrix} imn_\zeta \\ -i(\epsilon_\eta m+\gamma_1|m|) \\ \epsilon_\eta m+\epsilon_\xi|m| \\ 0 \end{pmatrix} \text{ and } \begin{pmatrix} -im^2 \\ -imn_\zeta \\ 0 \\ \epsilon_\eta m+\epsilon_\xi|m| \end{pmatrix}$$

which gives the surface impedance matrix for the origin as;

$$\begin{aligned} \begin{pmatrix} E_\eta \\ E_\zeta \end{pmatrix} &= \underline{\underline{\eta}} \begin{pmatrix} H_\eta \\ H_\zeta \end{pmatrix} \\ &= \frac{1}{\epsilon_\eta m+\epsilon_\xi|m|} \begin{pmatrix} imn_\zeta & -i\frac{m^2}{r} \\ -ir\frac{\epsilon_\eta m+\gamma_1|m|)}{|m|} & iimn_\zeta \end{pmatrix} \begin{pmatrix} H_\eta \\ H_\zeta \end{pmatrix} \end{aligned}$$

10.8 Power dissipation

The current carried by the particles is given by

$$\mathbf{J_p} = -i\underline{\underline{K}} \cdot \mathbf{E} + i\mathbf{E}$$

Swanson gives the volume power dissipation density as;

$$\begin{aligned}
D &= \mathrm{Re}(\mathbf{J_p} \cdot \mathbf{E}^*) \\
&= \mathrm{Re}\left[-i\left(\underline{\underline{K}} \cdot \mathbf{E}\right) \cdot \mathbf{E}^* + i\mathbf{E} \cdot \mathbf{E}^*\right] \\
&= \mathrm{Re}\left[-i\left(\underline{\underline{K}} \cdot \mathbf{E}\right) \cdot \mathbf{E}^*\right] \\
&= \mathrm{Re}\left[-i\begin{pmatrix} S & -iD & 0 \\ iD & S & 0 \\ 0 & 0 & P \end{pmatrix} \mathbf{E} \cdot \mathbf{E}^*\right] \\
&= \mathrm{Re}\left[-i\begin{pmatrix} SE_\xi - iDE_\eta \\ iDE_\xi + SE_\eta \\ PE_\zeta \end{pmatrix} \cdot \begin{pmatrix} E_\xi \\ E_\eta \\ E_\zeta \end{pmatrix}\right] \\
&= \mathrm{Re}\left[-i\left(SE_\xi E_\xi^* - iDE_\eta E_\xi^* + iDE_\xi E_\eta^* + SE_\eta E_\eta^* + PE_\zeta E_\zeta^*\right)\right] \\
&= \mathrm{Re}\left[-DE_\eta E_\xi^* + DE_\xi E_\eta^* - iPE_\zeta E_\zeta^*\right] \\
&= D\mathrm{Re}\left[-E_\eta E_\xi^* + E_\xi E_\eta^*\right] + \mathrm{Im}\left[P\right]|E_\zeta|^2 \\
&= D\mathrm{Re}\left[-E_\eta E_\xi^* + (E_\eta E_\xi^*)^*\right] + \mathrm{Im}\left[P\right]|E_\zeta|^2 \\
&= D\mathrm{Re}\left[2\mathrm{Im}(E_\eta E_\xi^*)\right] + \mathrm{Im}\left[P\right]|E_\zeta|^2 \\
&= \mathrm{Im}\left[P\right]|E_\zeta|^2
\end{aligned}$$

Where the S and D terms in the dielectric tensor are assumed to be real, and loss terms are included only in the P term (supplying a small imaginary component).

The parallel electric field E_ζ can be expressed in terms of the magnetic field components using;

$$E = i\kappa \nabla \times H$$

which, in terms of the local coordinates used here reduces to;

$$E_\zeta = i\kappa_\zeta \left(-n_e t a H_\xi + \frac{C^2}{r} H_\eta + H'_\eta + \chi'_p H_\zeta\right) \tag{74}$$

10.9 Rotate coordinates for the surface impedance matrix

The preceeding section gives the surface impedance matrix in (η, ζ) coordinates, whereas the calculations in the vacuum layer between plasma and wall are in (θ, z) coordinates. rotation between them is simply calculated as follows.

$$\begin{aligned}
\begin{pmatrix} E_\eta \\ E_\zeta \end{pmatrix} &= \underline{\underline{Z}} \begin{pmatrix} H_\eta \\ H_\zeta \end{pmatrix} \\
&= \begin{pmatrix} Z_{11} & Z_{12} \\ Z_{21} & Z_{22} \end{pmatrix} \begin{pmatrix} H_\eta \\ H_\zeta \end{pmatrix} \\
\begin{pmatrix} E_\theta \\ E_z \end{pmatrix} &= \begin{pmatrix} C & S \\ -S & C \end{pmatrix} \begin{pmatrix} Z_{11} & Z_{12} \\ Z_{21} & Z_{22} \end{pmatrix} \begin{pmatrix} C & S \\ -S & C \end{pmatrix}^{-1} \begin{pmatrix} H_\theta \\ H_z \end{pmatrix} \\
&= \begin{pmatrix} C^2 Z_{11} + SC(Z_{12} + Z_{21}) + S^2 Z_{22} & C^2 Z_{12} + SC(Z_{22} - Z_{11}) - S^2 Z_{21} \\ C^2 Z_{21} + SC(Z_{22} - Z_{11}) - S^2 Z_{12} & C^2 Z_{22} - SC(Z_{12} + Z_{21}) + S^2 Z_{11} \end{pmatrix} \begin{pmatrix} H_\theta \\ H_z \end{pmatrix}
\end{aligned}$$

11 Guide to the code

A program "nloops" has been written to perform the calculations outlined in this report. This section provides a short guide to the use of the code, and an introduction to its inner workings.

11.1 Compilation

The program code is written in standard fortran F77 and consists of some 25 files of subroutines. The same program source code is used on all machines, however since the CRAY, on which the program was developed, has as default 64 bit (8 byte) real numbers, on other machines such as ALPHA or SUN workstations the compiler option for default 8 byte reals must be used (e.g. -r8). The program makes extensive use of NAG library routines. Also, for use on different parallel platforms one or two special routines must be linked. Several simple UNIX shell scripts have been written to compile the program for use on some typical machines, but they may require some tailoring for each user. The supplied shell-scripts are:

1. **nloops.cray** : compiles the program for use on CRAY
2. **nloops.pvm** : compiles and distributes the program to a cluster of workstations running PVM "Parallel virtual machine" software.
3. **nloops.ksr** : compiles the program for use on the Kendal square shared memory parallel computer.
4. **nloops.ncube** : compiles the program for use on the hypercube parallel computer NCUBE.

11.2 Making a data file

The program reads all the data it needs to run from standard input. Normally one makes a file of input data and feeds this to the program. The data in the input file is in a series of Fortran NAMELIST statements. These appear in the following order;

1. **PVM** or **KSR** or nothing - control data : required only when the program is run on a PVM array or Kendal Square.
2. **MAIND** - control data for the program.
3. **VACUUMD** or **PLASMAD** or **BBDAT** - data for the surface impedance matrix.
4. **BZLOOPD** - data on the placement of the loops making up the antenna array.
5. **FEEDD** - data on how the loops are to be connected to sources.

where further **BZLOOPD** and **FEEDD** namelist entries can also be added. The variable names and their function is described in the following sections.

11.2.1 PVM

HOSTS : list of character strings of the addresses of the machines that make up the cluster; eg. 'alpha1',spcs.aug'. The list must be ended by a null string ' ' .
SPEED : list of numbers representing the average time needed for a particular job on each machine specifed above (used to allocate an appropriate workload to each machine).

11.2.2 KSR

NPROC : number of processors that will be used for the computation (if larger that the number available, then the number available is used).

11.2.3 MAIND

JSCAN : determines in what mode the program will run:
1 scan over frequencies.
2 scan over Alfvén resonance layer position (r_{alfven}/r_{plasma}).
3 read in dielectric tensor from a file.
4 scan over frequencies but use only the vacuum dielectric tensor.
NSCAN : number of values in a parameter scan.
SMIN, SMAX : minimum and maximum values in the parameter scan.

11.2.4 VACUUMD

Used when the surface impedance matrix is to be than without plasma (**JSCAN**=4).
RPOL : plasma radius
RTOR : major radius of the torus
MMX, NMX : maximum poloidal and toroidal mode number to be used.

11.2.5 PLASMAD

RROL, RTOR : minor and major radius of the plasma.
WN, SN, DNS, DNMAX : electron density profile of the plasma
$n(r) = \mathrm{DNMAX}(1-(r/x)^{\mathrm{WN}})e^{-(r/(x\mathrm{SN}))^2}$ where x is chosen to give $n(r)/n(r_p) = \mathrm{DNS}$.
WT, ST, DTS, DTMAX : electron temperature profile of the plasma
$T_e(r) = \mathrm{DTMAX}(1-(r/x)^{\mathrm{WT}})e^{-(r/(x\mathrm{ST}))^2}$ where x is chosen to give $T_e(r)/T_e(r_p) = \mathrm{DTS}$.
WQ,SQ,QMIN,QMAX : q profile of the plasma,
$q(r) = \mathrm{QMAX} - (\mathrm{QMAX}-\mathrm{QMIN})(1-(r/r_p)^{\mathrm{WQ}})e^{-(r/(r_p\mathrm{SQ}))^2}$
NMX, MMX : maximum toroidal and poloidal mode to be computed.
NMXA,MMXA : maximum toroidal and poroidal mode to be computed using the plasma.
PRPMX2 : if $n_\perp^2 r_p^2 >$ PRPMX2 then the vacuum calculation is done instead of the plasma.
ISMX : number of nodes in the radial direction used in calculating the wavefields in the plasma.
DEL : r/r_p value for the first node.
NTORUS : amount of symmetry in the toroidal direction, eg. for 32 antennas symmetrically around the tortus, NTORUS=32.
NRES : toroidal mode number of the Alfvén resonance layer used in the resonance layer scan.
HALL : logical variable turning the enhanced hall effect on.
DB0 : toroidal magnetic field.
DM : m_i/m_e
PSTOR : logical variable which controls the storing of the plasma calculations for later reconstruction of a power deposition profile (faster when .false.).

11.2.6 BBDAT

Used when the surface impedance matrix is to be read from a file (**JSCAN**=3).
ETAFILE : character string giving the filename of the file containing the plasma surface impedance matrix.

11.2.7 FEEDD

RSOURCE : array of Thevenin equivalent series source impedance of the sources on each antenna loop. Note e^{-iwt} convention!
USOURCE : array of Thevenin equivalent source voltage of the sources in each antenna loop.
RLINE : The impedance of the feed line. Used for calculations of the maximum expected line voltage in the feed line.

11.2.8 BZLOOPD

PMX : number of modes around each antenna loop.
KMX : number of terms in the power series for the inhomogeneous solution in the antenna region
LMX : number of loops in the antenna simulation.
PAIR :Logical flag. Place a loop π out of phase, toroidally opposite.
ESTOR : (Logical variable) store the electric fields at the plasma surface for each antenna and mode, for later reconstruction of the Poynting flux distribution in (n, m) space. Faster if .false..
R1, R2, RF, RW : radius of the front and back of the antenna loops and of the Faraday screen and vessel wall respectively.
SHEETS : logical varible truning on the current sheets at the plasma surface Faraday screen and wall.
ETABIG, TF : Surface resisitivity (ohms/square) of the Faraday screen in a direction perpendicular to the rods.
RHOF, RHOW, RHOA : Surface resistivity ohms/m of the Faraday screen, wall and antenna.
PHI0, Z0 : Arrays specifying the position of the centre of each of the loops making up the antenna.
PHI, Z : Arrays specifying the poloidal and toroidal half width of each loop making up the antenna.
D : Distance anticlockwise from the middle of the back of each antenna to the position of the slice generator.

11.2.9 Choice of typical values

Make sure that

1. sufficient terms are included in the power series for the electric field in the region of the antenna. Typically $k_{max} > c(r_2 - r_1)\sqrt{n_{max}^2/R^2 + m_{max}^2/r_p^2}$ with $c \approx 10$.

2. sufficient modes on the antenna are used to model the current distribution expected. The $\lambda/4$ resonance of a stripline antenna is modelled well with $p_{max} > 1$ or 2.

3. sufficient poloidal modes are used to resolve (a) the smallest poloidal feature of the antenna and (b) the highes mode computed on the smallest antenna loop: $m > 2\pi/\Phi_i$ and $m_{max}/r_2 > p_{max}/l_i$

4. sufficient toroidal modes are used to resolve the smallest toroidal feature on the antenna, eg between loops at least 1/2 wavelength. $n_{max}/R > 1/(2w_i)$

5. the plasma radius where the power series is used to compute the form of the fields near the origin should be small enough, but not smaller than 1 grid cell in the variational method. $\Delta > r_p/i_{max}$

6. enough radial grid points should be used to model the smallest feature in the wavefields (usually the Alfvén resonance layer) $r_p/i_{max} < \Delta_{\text{Alfvén}}$

11.3 Running the code

inputs:
(a) data file
(b) surface impedance matrix (when not to be calculated)
(c) special data for parallel machines.
outputs:
(a) power per loop - to standard output
(b) current distribution on each loop - to standard output
(c) radial power deposition profile - to file PR.RUNxx
(d) power deposited in each (m,n) mode - file SNM.RUNxx

11.4 Bugs and known problems

1. Memory limitations on NCUBE - The NCUBE allows only 4 Mbytes per node of which about 0.5 MByte is the operating system and 0.5 MBytes are required by the communications buffers, this limits operation to cases where relatively few radial grid-points or few antenna loops are to be calculated. When it is to be used only for antenna calculations, with the plasma surface impedance matrix coming from a file, this is not so much of a problem.

2. No power deposition profiles on KSR - Because of problems with the file handling on the KSR, storage of intermediate files is not possible.

3. Do not use too many antenna modes - if the poloidal wavelength implied by the maximum antenna mode number is larger than that representable by the highest poloidal mode computed, then some form of spectral pollution occurs.

4. Use enough terms in the power series - when insufficient terms of the power series in the antenna region are used to represent the most evanescent waves (high m,n), the partial impedance matrix is wrong.

5. When the first radial node is not close enough to the center, the assumptions used in the local power series are no longer true and a K_m like solution component appears and pollutes the first few nodes.

6. The enhanced Hall effect part of the code still doesnt work properly at low electron densities (results diverge). Run the code with **HALL** set to .false..

11.5 Use of the code together with M. Brambilla's code

Brambilla uses Gauss-CGS and only computes for a few poloidal and toroidal modes in "unfolded" plane geometry. A modified output routine "OUTDS2" generates a file with information on the poloidal and toroidal radii and the frequency, and lists the poloidal and toroidal modes computed. It then gives the surface impedance matrix for those modes (multiply by 120π to get MKSA units (ohms). The subroutine "BBILLA" reads in this file, interpolates to get the surface impedance for those modes not computed and converts to "dimensionless MKSA" (multiply by $\frac{1}{\mu_0 c}$).

11.6 Function of each subroutine

A brief outline of the purpose of each subroutine is given below.

nloops : This is the main program

size : an include file containing the maximum sizes to be used for the various arrays. The user should change these values as required.

nterms : Checks that sufficient terms have been included in the power series for the fields within the antenna.

bessels : Computes arrays of the Bessel functions required.

plasma : Calculates the plasma surface impedance matrix as outlined in this report and stores field profiles for later reconstruction of a power deposition profile.

hcm : Generates the matrix representing the variational form of the wave equations in the plasma.

hcf : Calculates the plasma parameter profiles and the dielectric tensor and calculates the terms $a_\zeta, a'_\zeta, a_{\zeta p}, a'_{\zeta p}, b_\zeta, b'_\zeta, b_{\zeta p}, b'_{\zeta p}, c_\zeta, c'_\zeta, c_{\zeta p}, c'_{\zeta p}$

fre1 : calculates the frequency at which the Alfvén resonance layer is at a particular radius.

bzloops : reads in the data defining the antenna array, and sets up some data to be used later in calculating the antenna fields.

bzloope : calculates the (m, n) Fourier component of the electric field of the p'th normal mode on the l'th loop, in presence of the plasma, Faraday screen and vessel wall.

bzloopz : calculates the matrix of partial impedances $Z_{pl}^{p'l''}$. Work on the different toroidal (n) modes is done in parallel.

jsheets : calculates the $\underline{\underline{M}}$ and $\underline{\underline{N}}$ matrices for use in calculating the image currents flowing in plasma, Faraday screen and vessel wall.

tayint : computes the $\int \sum_k (x-x_0)^k e^{ibx}\, dx$ used in the calculation of the Z from the antenna fields.

series : computes the local power series solution for the vacuum wave equations in the region of the antenna.

poly : evalulates a polynomial using Horners method.

diss : calculates the plasma dissipation profile for the next Fourier mode in the plasma fields file, given the surface electric field for that mode.

bwrite : writes the radial profile of E_ζ and ϵ_ζ for the (m, n) Fourier mode to a file.

cm1 : performs the volume integration on the cubic hermites.

cm2 : "

cip1 : "

bbilla : reads in the surface impedance matrix as calculated by M. Brambilla's program and interpolates between the values of m and n given.

nwork : decides whether a particular processor in the parallel machine should work on this task or wait for another one.

pvm.f : contains emulations of NCUBE parallel routines implemented using PVM subroutine calls.

ksr.f : contains emulations of NCUBE parallel routines implemented using Kendal Square subroutine calls.

serial : contains dummy emulations NCUBE subroutine calls to allow running on a simple serial machine.

11.7 Parallelization of the code

Further details can be obtained from [13]. The code was first written on the CRAY as a serial program and later moved to the NCUBE. The NCUBE offered the possibility to parallelize the program very simply by using a "HOSTLESS" parallel model. In this scheme the program is

loaded onto all (up to 64) processors identically and run. Each computer (node) reads a copy of the input data. At the parts in the program where a sum over toroidal mode n occurs, each node only works on a part of the summation, and results are collected at the end of the loop. This allowed parallelization with only 10 or 20 lines of changes in the entire program, and retained the understandability of the resulting program. Since the program is usually run with $n_{max} = 100$ resulting in 201 toroidal modes, this allows good distribution of computing load even on an NCUBE with 64 nodes.

Later, an array of very fast DEC-ALPHA workstations and several IBM RISC workstations became available, and it was decided to move parallelize the program to run on this cluster of workstations, which, at IPP, are all connected through the ETHERNET. Since the ratio between computation and data communication is very high for this program (as all n modes are totally independent), a virtual parallel machine using public domain software "PVM" and the network was practicable. The simplicity of the NCUBE parallel subroutines allowed the writing of routines named identically to those used by NCUBE, but using PVM subroutine calls internally.

Lastly a shared memory parallel computer "Kendal Square" became available and using the same philosophy as for PVM, a set of NCUBE look-alike routines was written using the KSR's parallel system calls.

12 Tests

12.1 Impedance of a loop in vacuum

Ideally we would like to use a configuration for which an exact analytic result was available for comparison, however the obvious choice of a circular loop would only involve the $m = 0$ mode, which was considered to be a little too restrictive. The compromise chosen was to model a small loop, roughly square in shape, extending poloidally and radially only a small distance.

12.1.1 Expected results

The theoretical results expected are:

1. A resonance i.e. $Z \to \infty$ when the loop circumference is about half the vacuum wavelength [10, p.250]

2. Well below the resonance frequency, the loop should act as an inductor of size

$$L = \frac{\mu_0}{\pi}\left(l_2 \text{cosh}_{-1}\frac{l_1}{d} + l_1 \text{cosh}_{-1}\frac{l_2}{d}\right)$$

[10, eqn.2-64] for a rectangular loop with sides l_1 and l_2 made with wire of diameter d, and where $d \ll l_1, l_2$. For a square loop os side length l, this reduces to,

$$L = \mu_0 \frac{2l}{\pi} \ln \frac{2l}{d}$$

3. When the loop perimeter is less than about $3/10\lambda$, the radiation resistance should be

$$R = 20\omega^4 S^2/c^4$$

where S is the area of the loop [10, eqn.2-57].

4. When $\text{Im}(Z) = 0$ there should be just over one wavelength around the loop. [10, p.250] gives, for $d = 0.001\lambda$ this point for 1.09λ and a radiation resistance of about 100 Ω.

5. When the loop is within a conducting wall the radiation resistance should be zero.

12.1.2 Numerical results

The parameters chosen for the computation were as follows, except where otherwise indicated on plots. For the following computations, the Faraday screen and the vessel wall are neglected, and the plasma surface impedance is replaced by the surface impedance in vacuum. Figure.1 gives the numercal results of this calculation.

R_{major}	=	$1.0m$	$\frac{1}{2}$width	=	$0.05m$
r_1	=	$0.80m$	m_{max}	=	20
r_2	=	$1.20m$	n_{max}	=	40
p_{max}	=	4	k_{max}	=	30

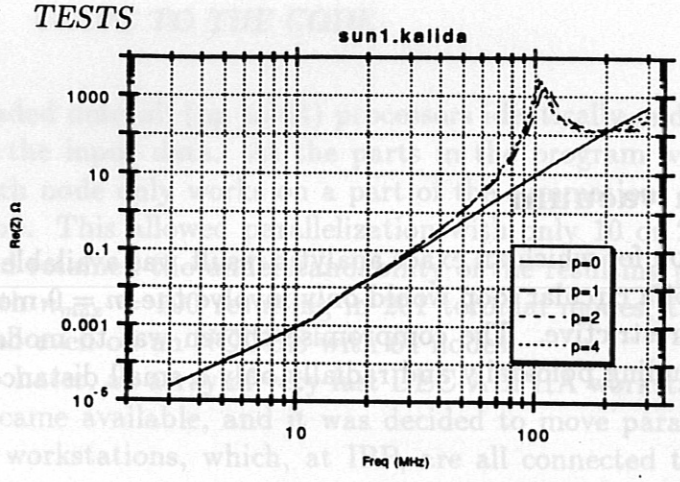

Figure 1: Calculated antenna resistance for a small loop as a function of frequency, showing convergence as the number of antenna modes increases

12.1.3 Discrepancies

The numerical results obtained highlighted several discrepancies between the model and the known results.

1. At low frequencies the radiation resistance scaled as f^3 instead of f^4. This unexpected result is really in agreement with the theory since what is being modelled is an infinite array of antennas, recalling that the toroidal geometry is simulated by having periodic boundary conditions in cylindrical geometry. It is found that increasing the separation between the loops, by increasing the major radius, decreases the frequency at which the antennas start to communicate too much.

2. When too many normal modes on the antenna are considered, the computed impedance is incorrect, showing spurious resonances. This unfortunate result is explained by noting that the electric field in the vicinity of the antenna, as a finite superposition of poloidal and toroidal normal modes, is an incomplete basis. When one specifies a source antenna current with much of its electric field in regions of (m,n) space not included in the computation, the partial impedances calculated for these modes will be in error.

3. Similarly, when insufficient terms in the series for the radial electric field are included, the corresponding partial impedance will be incorrect. Roughly, one should have more than $c(r_2 - r_1)\sqrt{n_{max}^2/R^2 + m^2/r^2}$ terms (with $c \approx 10$).

12.2 Impedance of a stripline in vacuum

A further simple test with known results is that of a stripline, where a thin conducting plate runs parallel to a groundplane. The appropriate geometry in this case is a loop with the radially outermost leg at the same radius as the conducting wall, and the innermost leg separated from the wall by a distance small compared to the wall radius. This ensures (i) the end effects due to the ends of the stripline are negligible and (ii) curvature effects can be neglected.

12.2.1 Expected results

1. The impedance should be that for a short circuited transmission line $Z = Z_0 \tan \beta l$ with a specific impedance (e.g. [11, 9-1]) and phase velocity that of light $\beta = \omega/c$

2. The current distribution should be flat in the central part of the conductor and peaked towards the edges, over a length of order the strip to wall separation.

12.2.2 Discrepancies

1. If the number of toroidal modes so small that the finite toroidal width of the individual strips modelling the full width of the stripline is not properly resolved. In this case we found that although the total current and hence impedance is correct, the current distribution is in error, with some strips even carrying negative current.

2. The effective length of the strap calculated is correct only to order Φ/m, i.e. as accurately as the poloidal modes allow resolution of the poloidal extent of the strap.

3. When the strap is poloidally short compared to its radial extent, the assumption that it is a transmission line fails, and it behaves more as a loop, showing an equivalent length equal to half the circumference. In this case the code also gives the correct answer compared to known results.

13 Results

13.1 Alfvén wave heating on Asdex Upgrade

An analysis of Alfvén wave heating possibilities on ASDEX upgrade was undertaken. The effect of the number of antennas, the antenna plasma separation, antenna limiters, and the effects of the current distribution on the antenna strap was considered. It is found that the image currents flowing in the antenna limiters severely degrade the antenna performance and that it is essential to have an antenna close to the plasma surface, exciting a toroidal mode $n = 12$ to 14.

On important detail is that since the most important aspect of the coupling is the radial evanescence of the fast wave between the antenna and the Alfvén wave resonance layer, and this depends upon the mode number launched. The major radius of the plasma should not be taken as the physical major radius of the torus, (1.65m) but as 2.15m, the major radius at the antenna. This explains the apparent discrepancy between the optimal n calculated by Puri [1, 2, 4] and that calculated here. Because of the elongation of the ASDEX upgrade plasma, $b/a = 0.64/0.5$ the plasma radius was taken as the vertical radius b and the resonance layer placed at r/b=0.609 to give a distance to the plasma-edge the same as that of a resonance layer at $r/a = 0.5$ in the horizontal plane.

13.1.1 Effect of antenna current distribution and limiters

The following figures show the Q, resistance and reactance of each antenna strap as a function of the number of pairs of antenna, assumed to be alternately out of phase and uniformly around the vessel. The launch freqency adjusted to keep the $(n, -1)$ Alfvén resonance layer at fixed position.

The calculations are made for 4 antenna structures.

1. A simple strap antenna with a uniform current distribution across it.
2. Modeling the strap by 3 sub-straps in parallel, to allow for peaking of the antenna current across the strap.
3. Additionally having two short circuited straps at +/-15cm around each strap to represent the image currents flowing in antenna limiters.
4. Moving these limiters to +/-20cm.

The most obvious feature in the graph (fig.2) of antenna Q as a function of n is the well defined minumum around $n = 10$. As has been well documented earlier by Puri this results from a tradeoff between the strongly decreased loading at higher n due to the increased radial evanesence of the wave, and the decreased confluence between the fast and slow wave at low n.

The effect of the correct antenna current distribution across the strap is to peak the current towards the edge, increase the proportion of the antenna flux at higher n harmonics and decrease the amount in n. Thus we see a small decrease in the resistive part of the loading (fig.4). However the reactive part of the loading (fig.3) decreases much more, and the antenna Q is overall reduced by 10%. At $n = 10$ about 1/3 of the current flows in each edge of the antenna strap.

When antenna limiters are included into the calculation, the antenna reactance is strongly decreased, however the antenna resistive loading is even more strongly reduced, and the antenna Q rises by about 1.5 at the optimal n for the +/-20cm limiter case, and over a factor 2.5 for the +/-15cm limiter case. At $n = 10$ with limiters at +/- 20cm the image currents are reduced to about 1/6 of the strap current flows in each limiter. These results suggest that it is important to minimize the eddy currents flowing in the antenna limiters.

The power deposition profiles are seen to have more power deposited in the edge regions when arrays launching prodominantly low n modes (figs. 5 to 7) are used. This results from other poloidal modes, which for low n have resonance layers further separated from the $m = -1$ mode,and hence closer to the plasma edge.

13.1.2 Effect of antenna-plasma separation

The figure.8 shows the antenna Q as a function of n for several antenna-plasma separations. The antenna Q increases strongly with increasing spearation, however the low n configuration have a weaker dependence on n because of the lesser radial evanescence of the fast wave ($k_\perp^2 \approx -(n/R)^2 - (m/r)^2$ in vacuum). The number of antenna pairs (n) giving the lowest Q is also found to be a function of the antenna-plasma gap, shifting from $n = 10$ for a 15cm gap to $n = 13$ for a 1cm gap. This results from a shift in the tradeoff between the evanescence in the edge and the wave damping, since for very large gaps, the evanescents assumes a greater role, and for small gaps the mode damping is more important.

13.1.3 Parameters used for calculation

JSCAN=2 NSCAN=1 SMIN=0.609375 SMAX=1.0 RTOR=2.15 NMX=100 NMXA=32
RPOL=0.64 MMX=20 MMXA=10 ISMX=1000 DEL=0.002 PRPMX2=-1.0E20
NTORUS=1 NRES=1 HALL=.FALSE. PSTOR=.TRUE. DBO=2.5 DM=1822.88
WN=4.0 SN=20.0 DNS=0.01 DNMAX=2.0E20
WT=2.0 ST=20.0 DTS=0.01 TEMAX=4000.0
WQ=2.0 SQ=20.0 QMIN=1.0 QMAX=3.0
PMX=2 KMX=80 PAIR=.TRUE. ESTOR=.TRUE. R1=0.74 R2=0.94 RF=0.68 RW=0.94
SHEETS=.TRUE. ETABIG=1.0E20 TF=0.0 RHOF=1.0E80 RHOW=0.0 RHOA=0.0
For a an antenna with uniform current density in z.
RSOURCE=(0.,0.) USOURCE=(1.,0.) PHI0=0.00 PHI=27.2837 D=0.47143 LMX=1 Z=0.1
Z0=0.
For a an antenna with varying current density in z.
RSOURCE=3*(0.,0.) USOURCE=3*(1.,0.) PHI0=3*0.00 PHI=3*27.2837, D=3*0.47143 LMX=3
Z=0.02 0.06 0.02 Z0=-0.08 0.0 0.08
For a an antenna with varying current density in z and side limiters.
RSOURCE=5*(0.,0.) USOURCE=(0.,0.) 3*(1.,0.) (0.,0.) PHI0=5*0.00 PHI=5*27.2837,
D=0.0, 3*0.47143 0.0 LMX=5 Z=0.01 0.02 0.06 0.02, 0.01 Z0=-0.15 -0.08 0.0, 0.08, 0.15

13.2 Alfvén wave current drive on Asdex Upgrade

Alfvén waves are thought to be an efficient method for driving the toroidal current in tokamaks, due to their low phase velocity, where they can couple to the sub thermal electrons. Here we present some calculations for the ASDEX upgrade tokamak. An array of 32 antennas is assumed, phased to drive the $n = +8$ mode. Antennas of width 20cm, length 80cm and depth 20cm are assumed and the Alfvén resonance layer is put at $r/a = 0.7396$ to give a resonance layer at the same distance from the plasma edge as at $r/a = 0.66$ in the horizontal plane.

The radial profile of the power dissipation 9 shows a very well localized deposition of power, the antenna Q is calculated to be 29.2 and the reactance 4.96 ohms (at 2.56 MHz). Because the antenna straps are only 422mm apart and are 200mm wide, most of the current is found to flow in the edge regions of each strap and the assumption of a uniform current density is found to give quite a larger inductance and a worse antenna performance, X =6.8 ohms and Q =31.5. An interesting observation is that because the antenna array is launching a travelling wave, the down-stream side of each antenna strap appears to absorb a large proportion of the power launched by the up-stream side of the antenna (recall that the current distribution on the strap is modelled by have several thin straps in parallel). For a total launched power of 1 MW the voltage on each antenna is 8.6kV.

13.2.1 Parameters used for the calculation

JSCAN=2 NSCAN=1 SMIN=0.73958 SMAX=1.0 RTOR=2.15 NMX=64 NMXA=32 RPOL=0.64
MMX=20, MMXA=10 ISMX=1000 DEL=0.02 PRPMX2=-1.0E20 NTORUS=8, NRES=8
HALL=.FALSE. PSTOR=.TRUE. DBO=2.5 DM=1822.88
WN=4.0 SN=20.0 DNS=0.01 DNMAX=2.0E20 WT=2.0 ST=20.0 DTS=0.01 TEMAX=4000.0
WQ=2.0 SQ=20.0 QMIN=1.0 QMAX=3.0 ETAFILE=' ',
RSOURCE=6*(0.,0.) USOURCE=3*(1.,0.) 3*(0.,1.) PMX=3 KMX=65 LMX=6 PAIR=.TRUE.
ESTOR=.TRUE. R1=0.74 R2=0.94 RF=0.69 RW=0.94, SHEETS=.TRUE. ETABIG=1.0E20
TF=0.0 RHOF=1.0E80 RHOW=0.0 RHOA=0.0
PHI0=6*0.00 PHI=6*27.2837 D=6*0.44762 Z=0.02 0.06 0.02 0.02 0.06 0.02 Z0=-0.080 0.000
0.080 0.34215 0.42215 0.50215

13.3 The 1993 ICRH antenna on Asdex Upgrade

The ICRH antennas currently used on ASDEX upgrade were also modelled by the code presented here. Typical ASDEX upgrade parameters for the H minority heating scenario, and the effects of the current distribution across the antenna strap and the effects of the antenna side limiters was modelled. An antenna consisting of four equal loops of size equal to the average loop size on AUG are used.

The effect of accounting for the correct current distribution across the strap is to reduce the effective inductance of the antenna by 15%, and the effect of the limiters and the septum is to reduce the inductance by 30% in the case of in phase straps. This changes the resonant frequency calculated for the antenna, so direct comparisons between the models are not entirely clear.

	$2P/I^2_{short}$
π phasing , J uniform	3.62
π phasing , J correct	1.60
π phasing , with limiters	2.57
0 phasing , J uniform	2.61
0 phasing , J correct	2.03
0 phasing , with limiters	2.33

The resisitive loading results (representend by an equivalent series resistance at the short circuited end of the strap), shows that the effect of considering the current distribution across the strap reduces the loading, and that including the limiters and septum gives a value in between, for both 0 and π strap phasings. This is in contrast to the AWH case where limiters decreased the loading. In this case the image currents flowing in the limiters presumably add to that part of the spectrum with good absorbsion.

13.3.1 Parameters used for the calculation

ETAFILE='/uts/ceh/felice/f30n80m40' PMX=4 KMX=85
PAIR=.FALSE. ESTOR=.TRUE. LMX=4 R1=0.88 R2=1.03 RF=0.86 RW=1.03
SHEETS=.TRUE. ETABIG=1.0E20 TF=0.0 RHOF=0.0 RHOW=0.0 RHOA=0.0
For uniform currents on across each strap,
RSOURCE=4*(0.,0.) USOURCE=(-1.,0.) (1.,0.) (-1.,0.) (1.,0.) PHI0=2*14.0 2*-14.0
PHI=4*13.0 Z=4*0.09 Z0=-0.18 0.18 -0.18 0.18 D=4*-0.24
For varying currents on across each strap,
RSOURCE=12*(0.,0.) USOURCE=3*(1.,0.) 3*(-1.,0.) 3*(1.,0.) 3*(-1.,0.)
PHI0=6*14.0 6*-14.0 PHI=12*13.0 D=12*-0.24
Z=0.02 0.05 0.02 0.02 0.05 0.02 0.02 0.05 0.02 0.02 0.05 0.02
Z0=-0.25 -0.18 -0.11 0.11 0.18 0.25 -0.25 -0.18 -0.11 0.11 0.18 0.25
For varying currents on across each strap with side limiters and septum,
RSOURCE=18*(0.,0.) USOURCE=3*(1.,0.) 3*(-1.,0.) 3*(1.,0.) 3*(-1.,0.) 6*(0.,0.)
PHI0=6*14.0 6*-14.0 3*14.0 3*-14.0 PHI=18*13.0 D=12*-0.24 6*0.
Z=0.02 0.05 0.02 0.02 0.05 0.02 0.02 0.05 0.02 0.02 0.05 0.02 6*0.02
Z0=-0.25 -0.18 -0.11 0.11 0.18 0.25 -0.25 -0.18 -0.11 0.11 0.18 0.25 -0.35 0.0 0.35 -0.35 0.0 0.35

13.4 Proposed "Violin" antenna for ITER

In the JET report [17] a new type of antenna is suggested for use on ITER. It consists of a single poloidal strap 3m in length, earthed at each end to the vessel wall and fed from a 30 ohm coaxial line 0.4m from the upper end. It is thus a poloidally asymmetric antenna. One proposed advantage of the antenna is that the antenna loop is self supporting and can support the central conductor of the coaxial line, thus relieving the need for ceramic supports in the vicinity of the plasma. A second proposed advantage is that the short 0.4m loop will act as a parallel addmitance and help to match the reactive load of the antenna since the relatively long 2.6m strap will have several resonances in the frequency range of interest (20-100MHz), and this provides several positions where antenna should be almost matched by the short loop.

The program detailed in this report was used to model some features of this antenna. Because the Faraday screen is modelled as sheet of anisotropic conductivity, and is not restricted to the antenna region, it can and does support coaxial modes which propagate between the Faraday screen and the wall as though the Faraday screen was the central conductor and the wall the outer conductor. This effectively means that the extra capacitive loading given by the Faraday screen disappears in the model when there is one wavelength around the torus. Since a freqency scan was to be performed for the antenna, a pair of π phased antennas 70.5 cm apart was modeled in order to circumvent this probelm.

1. It is wrong to consider the two straps as sections of transmission line with a phase determined by their length in the toroidal direction. Figure.10 shows the current flowing in the two arms of the antenna as a function of frequency. It is found that the quarter wavelength resonances of each loop are consistent with assuming length of the equivalent stripline is about 35cm longer than the poloidal length. This can be considered as due to the extra inductance of the radial feed sections which is not included inthe JET report. This does not have a large effect on the longer arm, but represents nearly a factor of 2 for the smaller loop. This is an advantage in that the short loop can be made much shorter in the poloidal direction to achieve the same effect as reported in the JET report. Since, as will be seen later the effect of the counter flowing current in the short arm is to reduce the loading by coupling power out of the wave, it is better when this loop is smaller.

2. The small 40cm "matching" loop, does not, as reported by the JET report, contribute to the antenna loading, rather, power is absorbed by this loop and decreases the effective antenna loading. Using a plasma surface impedance for typical ITER plasmas supplied by Brambilla it is found that at 30 MHz about 25

3. The calculated voltages in the 30 ohm transmission line feeding the loops was 24.4 kV for 2MW on the 2 antennas. Although a direct comparison was difficult because of the incorrect electrical lengths used in [17], if one adjusts the frequency a little to give the same reactances in the longer strap, then the line voltages calculated here are 40% larger than in [17]. This may be partly due to the rather coarse "correction" but will also be due to the effect of having a reversal in the current on the longer strap, which should lead to a decrease in the loading in the same way as the counter flowing current in the short, 40cm strap.

13.4.1 Parameters used for the calculation

JSCAN=4 (vacuum) or 3(brambilla's plasma) NSCAN=30 SMIN=2.0E6 SMAX=60.0E6
RTOR=7.75 NMX=90 RPOL=4.48 MMX=60 ETAFILE='/uts/ceh/felice/f30n90m60'
RLINE=30.0 RSOURCE=4*(0.,0.) USOURCE=(1.,0.) (-1.,0.) (-1.,0.) (1.,0.)
PMX=3 KMX=85 LMX=4 PAIR=.FALSE. ESTOR=.TRUE.
R1=4.68 R2=4.93 RF=4.67 RW=4.93 SHEETS=.TRUE. ETABIG=1.0E10 TF=0.0 RHOF=0.0

RHOW=0.0 RHOA=0.0
PHI0=2*2.3848 2*-15.5014 PHI=2*2.3848 2*15.5014 Z=4*0.10
Z0=0.0 0.705 0.0 0.705 D=2*-0.2052 2*1.334

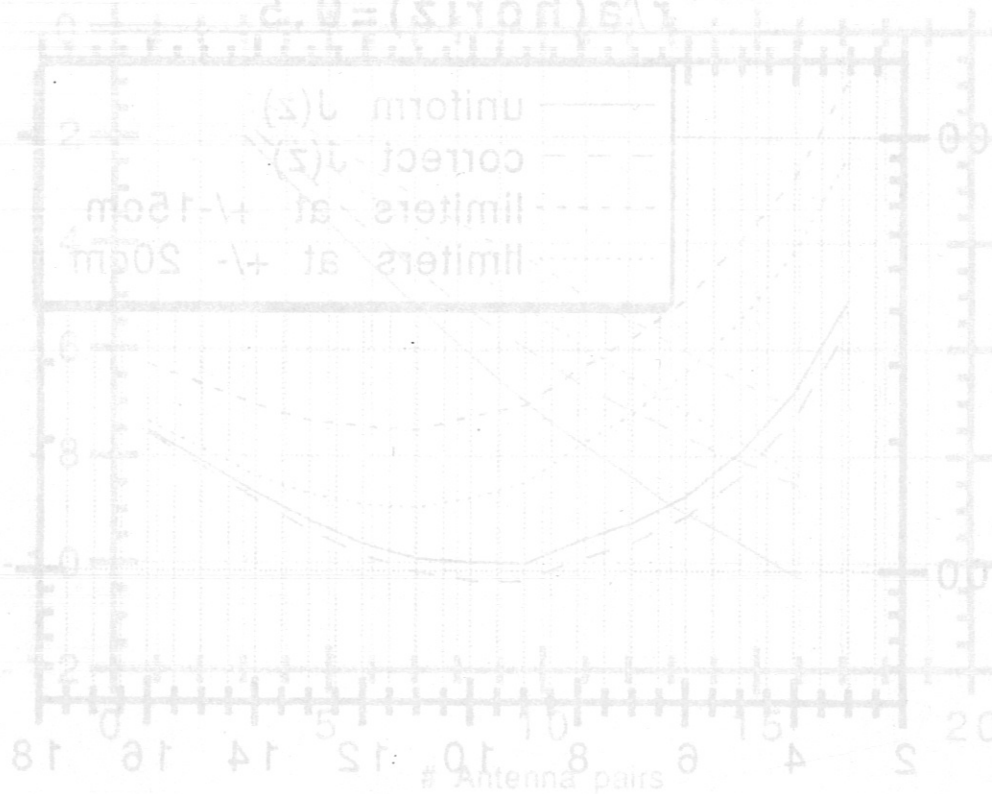

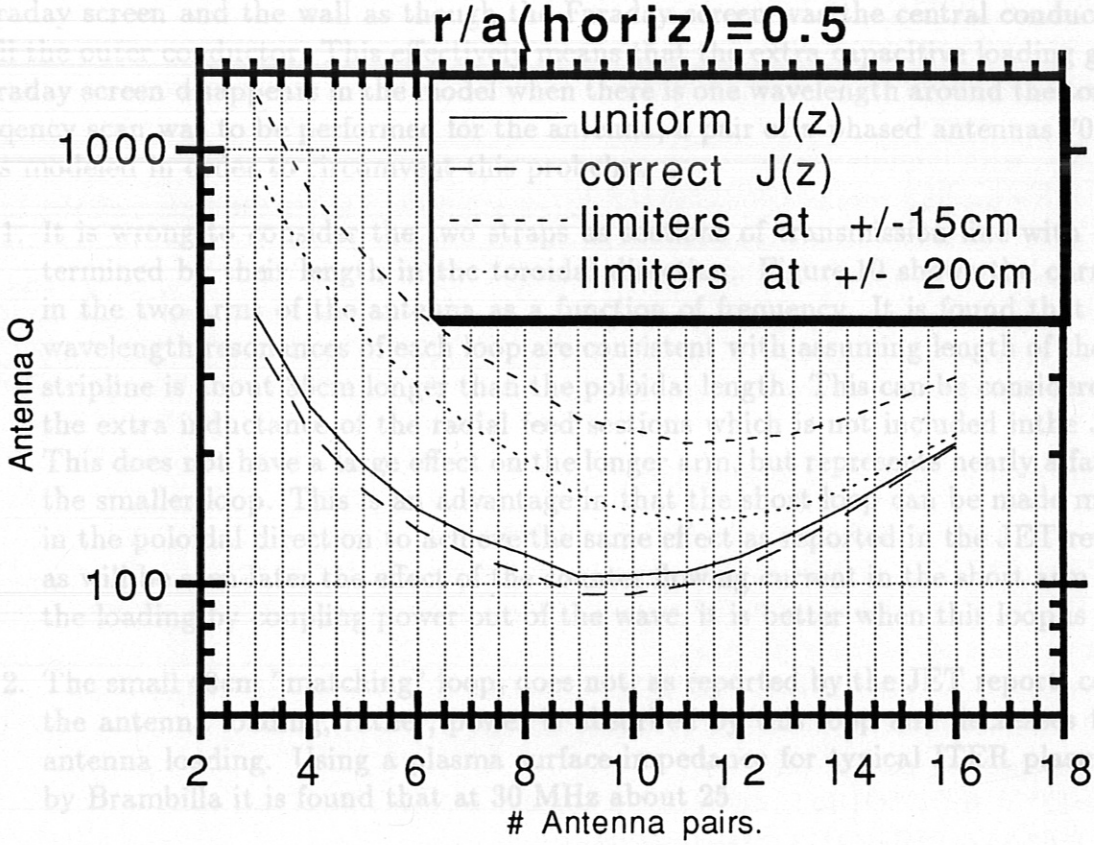

Figure 2: Antenna Q as a function of the number of antenna pairs, for 4 types of antenna model

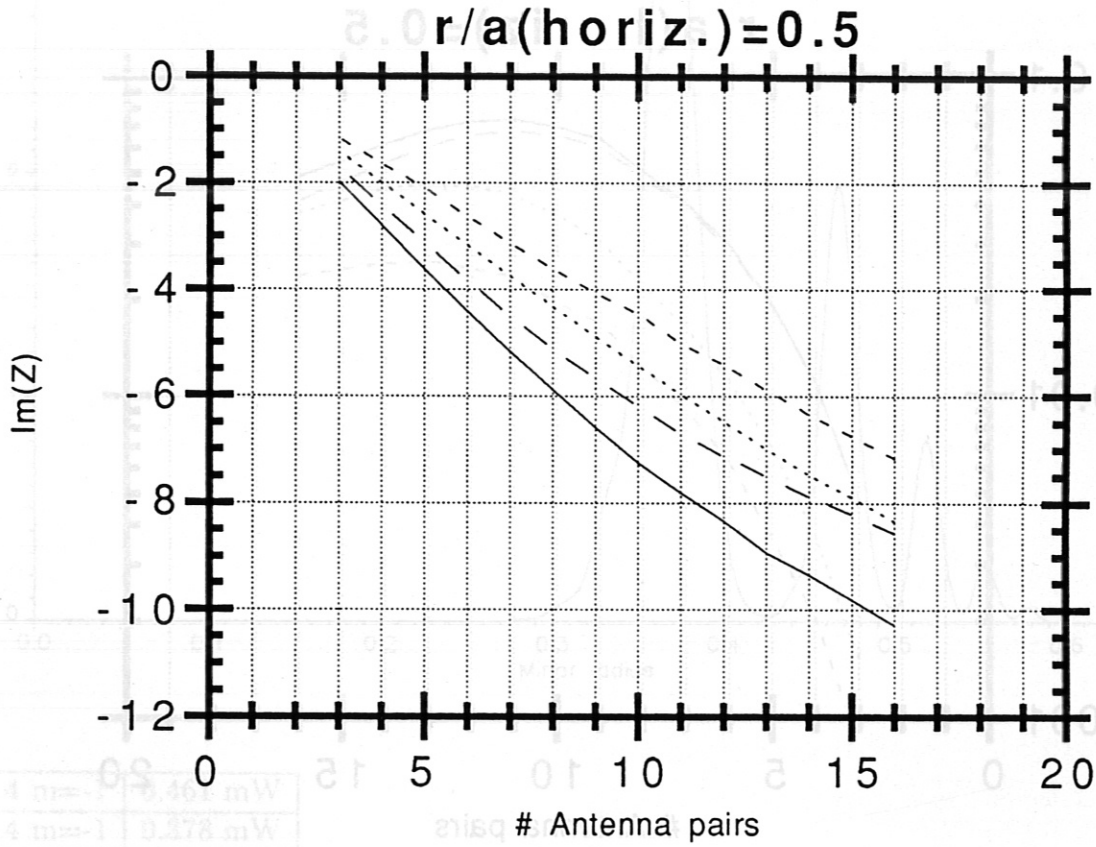

Figure 3: Antenna reactance as a function of the number of antenna pairs, for 4 types of antenna model

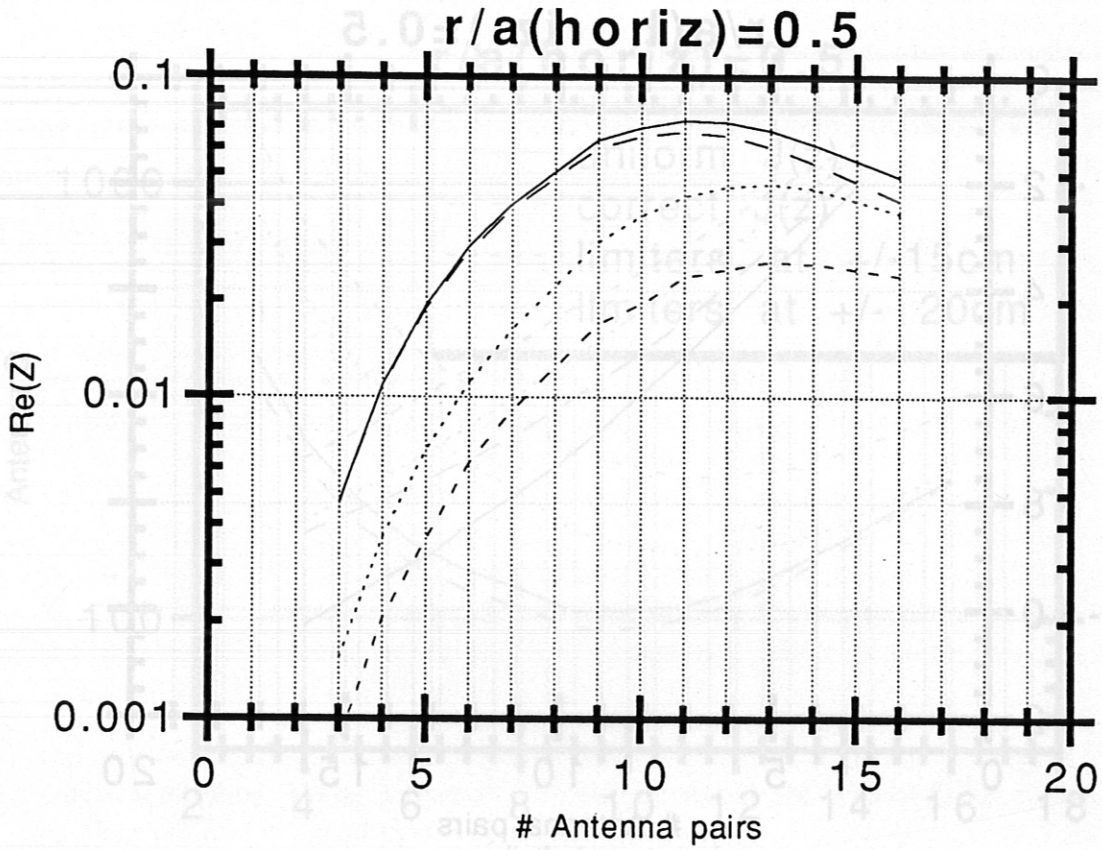

Figure 4: Antenna resistance as a function of the number of antenna pairs, for 4 types of antenna model

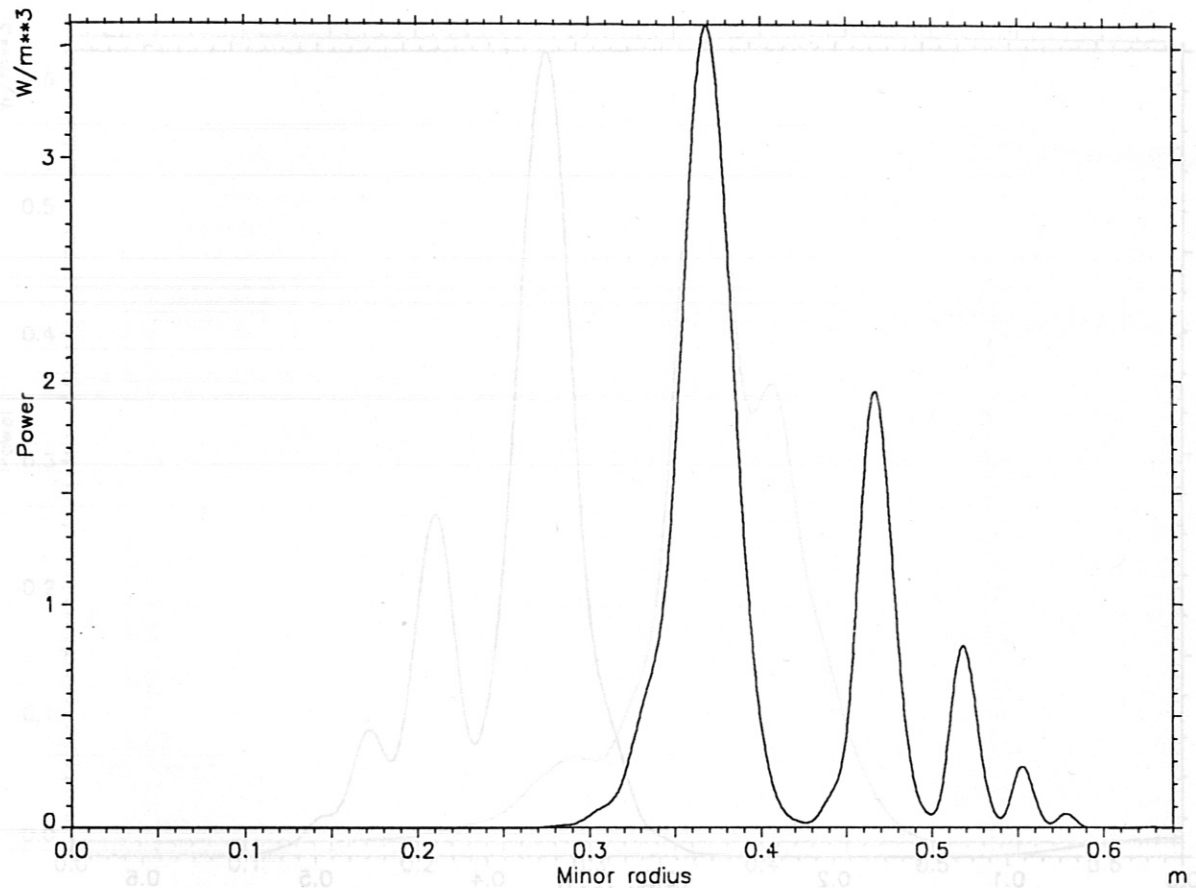

n= 4 m=-1	0.461 mW
n=-4 m=-1	0.378 mW
n= 4 m=-2	0.199 mW
n=-4 m= 2	0.169 mW
n= 4 m=-3	0.068 mW
n=-4 m= 3	0.059 mW
n= 4 m=-4	0.019 mW
n=-4 m= 4	0.011 mW

Figure 5: Radial power deposition profile for $n = 4$ for the simple strap antenna and 1 V on the antenna. Table of modes with dominant power absorbsion.

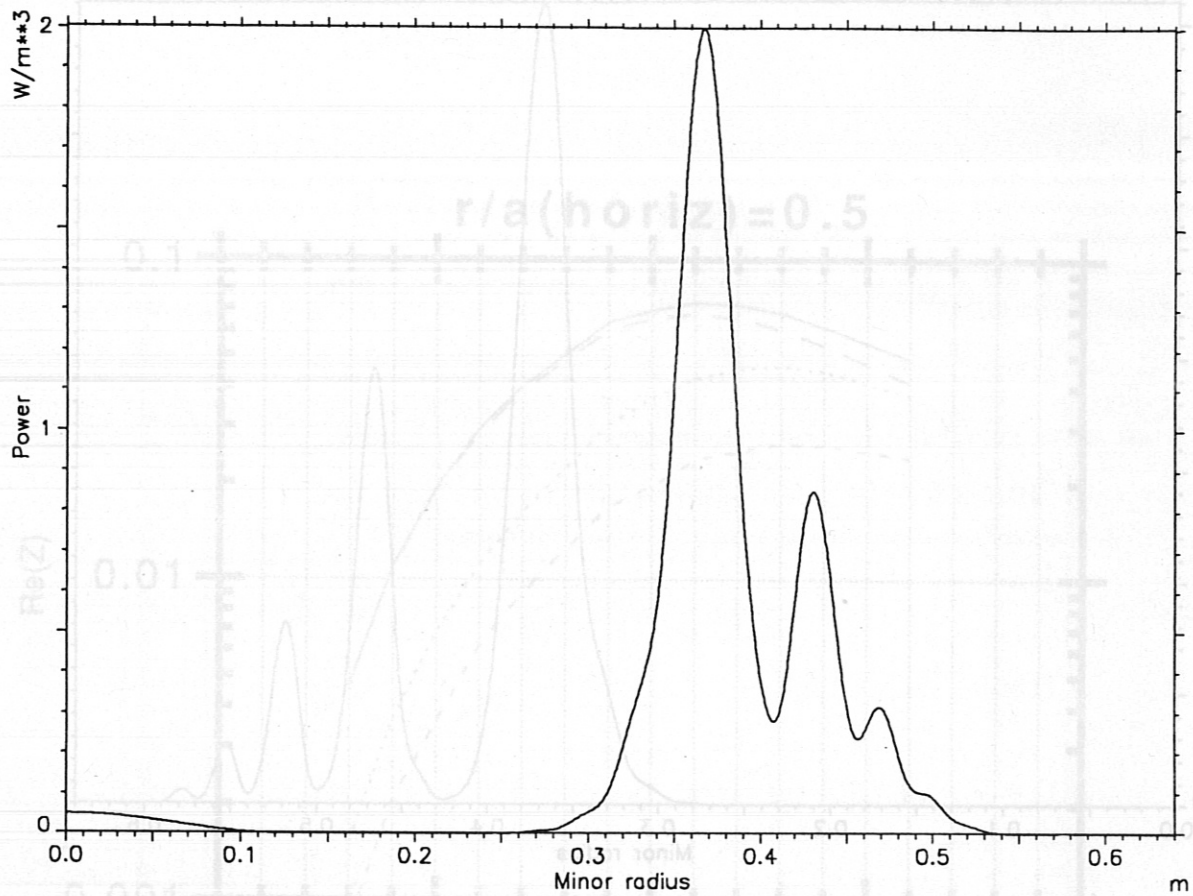

n= 8 m=-1	0.661 mW
n=-8 m=-1	0.273 mW
n= 8 m=-2	0.215 mW
n=-8 m= 2	0.125 mW
n= 8 m=-3	0.066 mW
n=-8 m= 3	0.043 mW
n= 8 m=-4	0.017 mW
n=-8 m= 4	0.011 mW

Figure 6: Radial power deposition profile for $n = 8$ for the simple strap antenna and 1 V on the antenna. Table of modes with dominant power absorbsion.

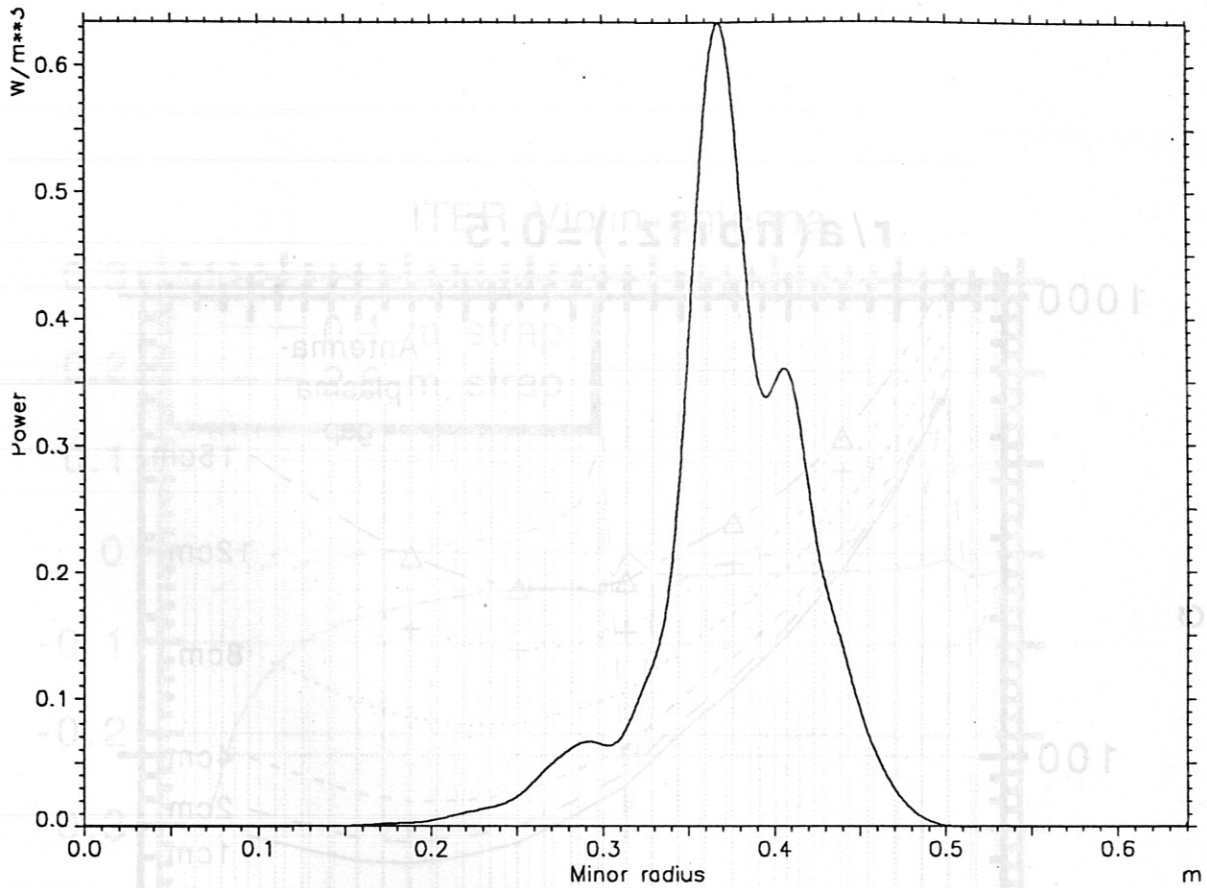

n= 14 m=-1	0.309 mW
n= 14 m=-2	0.138 mW
n=-14 m= 1	0.062 mW
n= 14 m=-3	0.040 mW
n= 14 m= 0	0.036 mW
n=-14 m= 2	0.034 mW
n=-14 m= 3	0.013 mW
n= 14 m=-4	0.010 mW

Figure 7: Radial power deposition profile for $n = 14$ for the simple strap antenna and 1 V on the antenna. Table of modes with dominant power absorbsion.

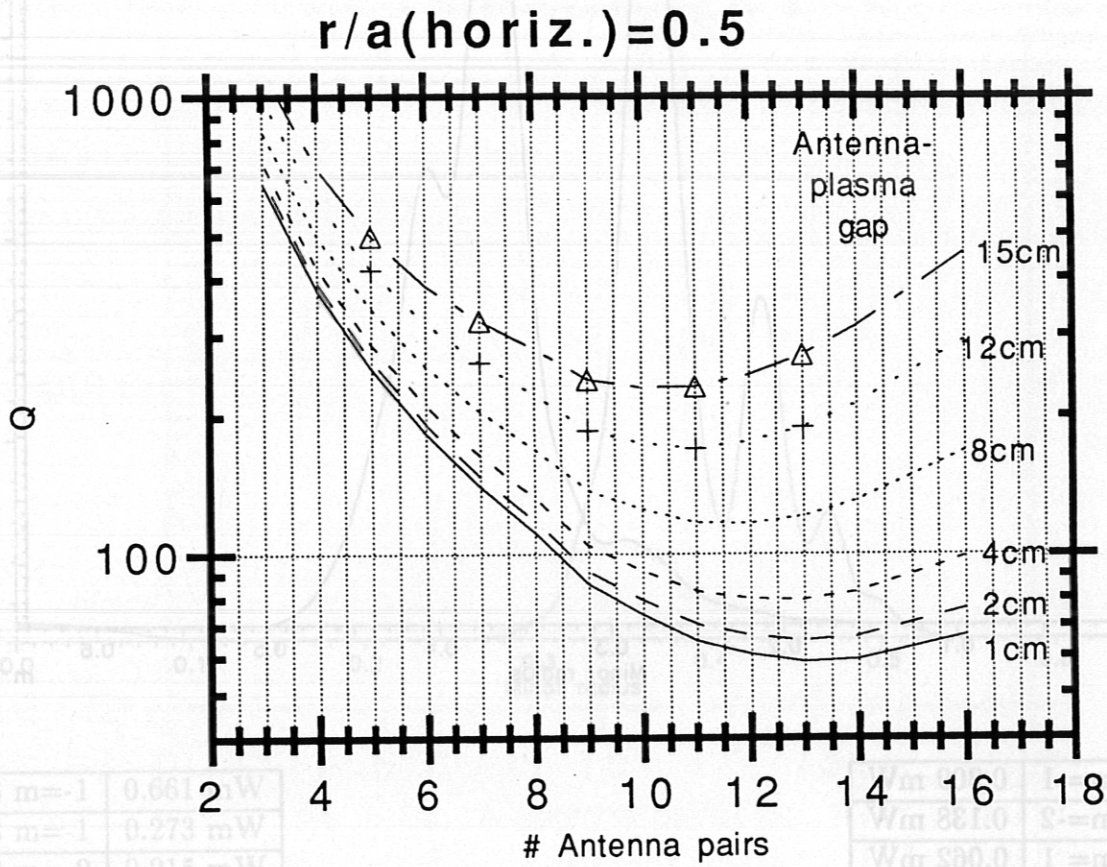

Figure 8: Antenna Q for an antenna with side limiters at +/-20cm as a function of the antenna to plasma edge gap

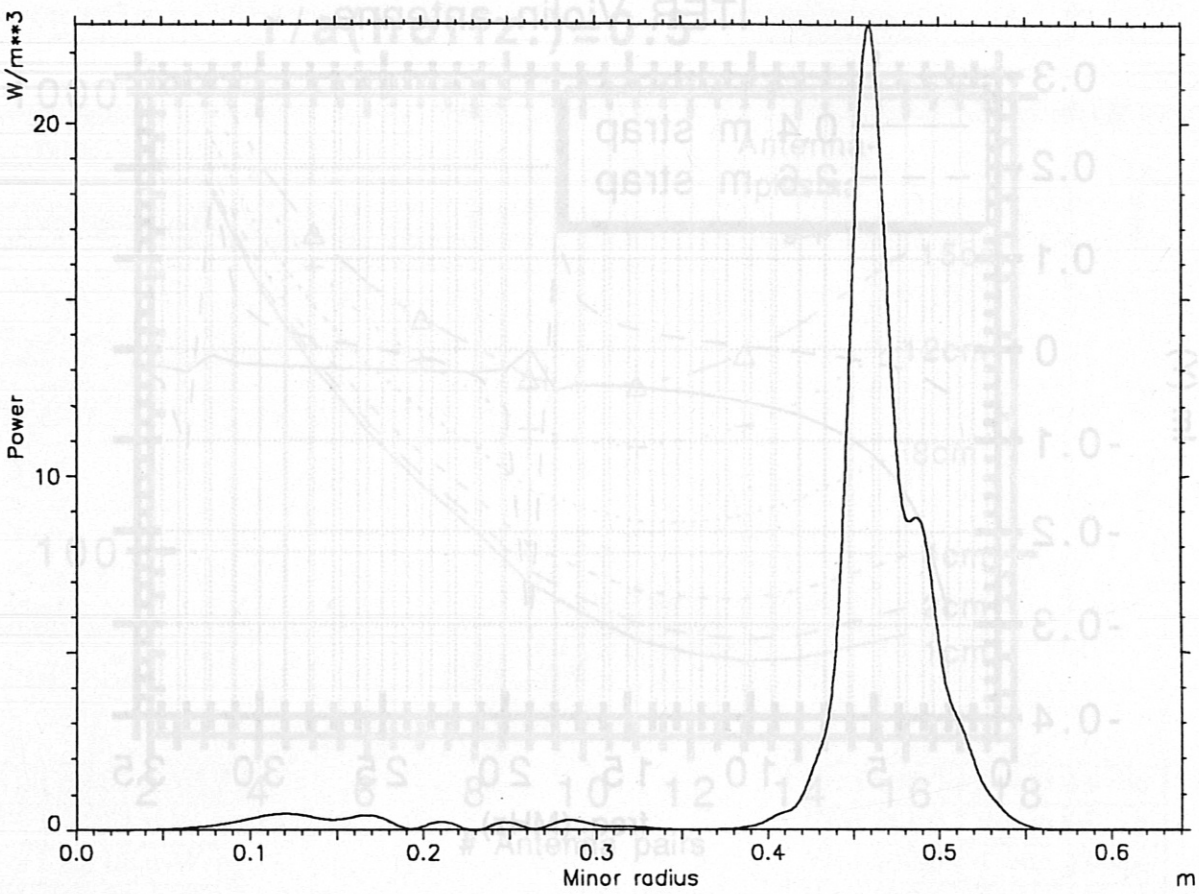

Figure 9: Radial power deposition profile for an array of 32 antennas launching the $n = +8$ mode.

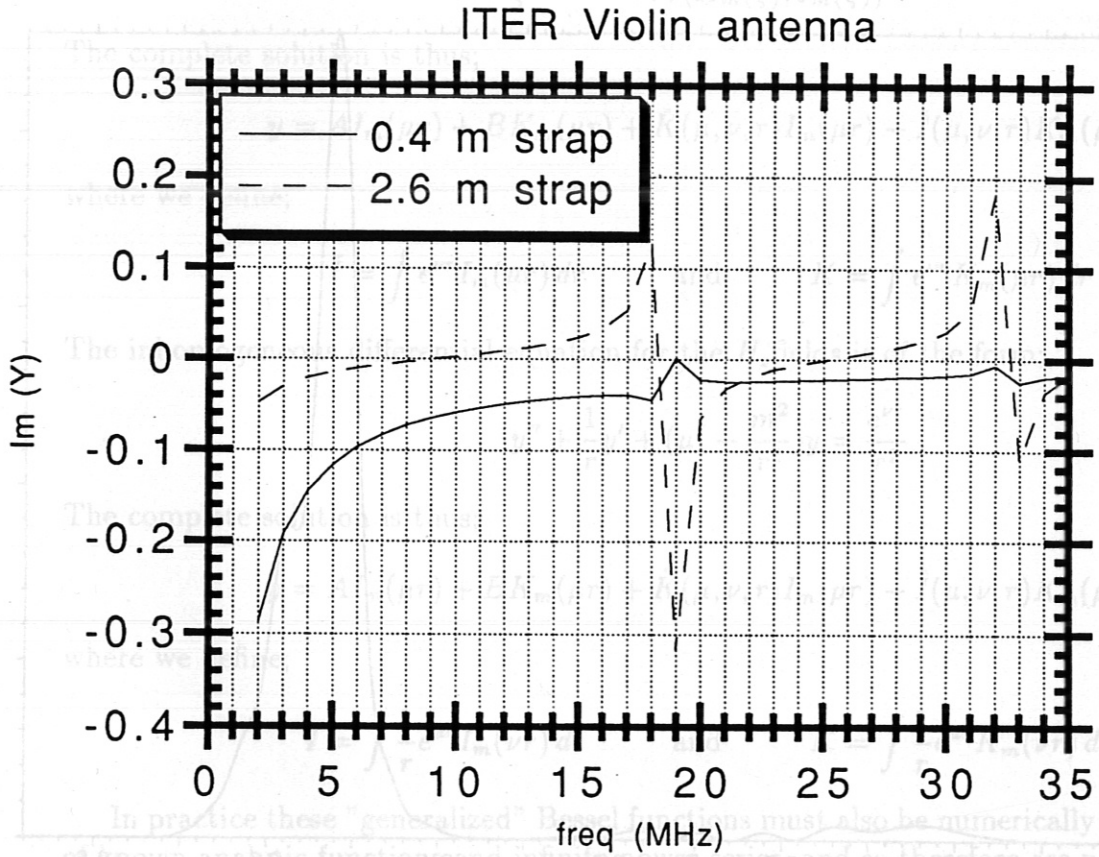

Figure 10: Current flowing from the source to each of the 2 straps as a function of frequency (vacuum calculation) for the proposed ITER "violin" antenna

14 APPENDIX: Computation of integrals

Although in the present version of this calculation the solution to the inhomogeneous wave equation (due to the radial volume currents) is achieved using a power series, it is useful to note that the inhomogeneous equation can be solved analyticaly in terms of some more generalized Bessel functions. The inhomogeneous differential equation for the $E_z$fields is of the form;

$$y'' + \frac{1}{r}y' + (\mu^2 - \frac{m^2}{r^2})y = \frac{e^{\nu r}}{r}$$

giving the particular solution (from [16](eq.55))

$$y = \int^r \frac{e^{\nu\zeta}}{\zeta} \frac{K_m(\mu\zeta)I_m(\mu r) - I_m(\mu r)K_m(\mu\zeta)}{\mathcal{W}(K_m(\zeta), I_m(\zeta))}\, d\zeta$$

The complete solution is thus;

$$y = AI_m(\mu r) + BK_m(\mu r) + \check{K}(\mu,\nu,r)I_m(\mu r) - \check{I}(\mu,\nu,r)K_m(\mu,r)$$

where we define;

$$\check{I} = \int e^{\nu r} I_m(\mu r)\, dr \qquad \text{and} \qquad \check{K} = \int e^{\nu r} K_m(\mu r)\, dr$$

The inhomogeneous differential equation for the $H_z$fields is of the form;

$$y'' + \frac{1}{r}y' + (\mu^2 - \frac{m^2}{r^2})y = \frac{e^{\nu r}}{r^2}$$

The complete solution is thus;

$$y = AI_m(\mu r) + BK_m(\mu r) + \hat{K}(\mu,\nu,r)I_m(\mu r) - \hat{I}(\mu,\nu,r)K_m(\mu,r)$$

where we define;

$$\check{I} = \int \frac{1}{r} e^{\mu r} I_m(\nu r)\, dr \qquad \text{and} \qquad \check{K} = \int \frac{1}{r} e^{\mu r} K_m(\nu r)\, dr$$

In practice these "generalized" Bessel functions must also be numerically evaluated in terms of known analytic functions and infinite power series, and so therefore are no more useful than the simple direct power series solution. However in some case they converge much faster, because some exponential like factors are removed from the power series, and so they may be useful for future optimization of the calculation of the antenna field.

14.1 Integrals of the form $\int e^{az} z^n dz$

$$I_0 = \int e^{az} dz = \frac{e^{az}}{a}$$

$$\begin{aligned} I_1 &= \int e^{az} z dz = z\frac{e^{az}}{a} - \int \frac{e^{az}}{a} dz \\ &= \frac{e^{az}}{a^2}(az - 1) \end{aligned}$$

$$\begin{aligned} I_n &= \int e^{az} z^n dz \\ &= \frac{1}{a} e^{az} z^n - \int \frac{n}{a} e^{az} z^{n-1} dz \\ &= \frac{1}{a} e^{az} z^n - \frac{n}{a} I_{n-1} \end{aligned}$$

We conjecture that;

$$I_n = \frac{e^{az}}{a^{n+1}} n!(-1)^n \sum_{k=0}^{n} \frac{(-az)^k}{k!}$$

The cases $n = 0$ and $n = 1$ are immediately seen to be true. Considering the case $n + 1$ we have,

$$\begin{aligned} \mathrm{RHS}_{n+1} &= \frac{e^{az}}{a^{n+2}} (n+1)!(-1)^{n+1} \sum_{k=0}^{n+1} \frac{(-az)^k}{k!} \\ &= \frac{1}{a} \frac{e^{az}}{a^{n+1}} \left[-(n+1)n!(-1)^n \left(\sum_{k=0}^{n} \frac{(-az)^k}{k!} + \frac{(-az)^{n+1}}{(n+1)!} \right) \right] \\ &= \frac{n+1}{a} I_n + \frac{1}{a} \frac{e^{az}}{a^{n+1}} (n+1)n!(-1)^n \frac{(-az)^{n+1}}{(n+1)!} \\ &= \frac{e^{az}}{a} z^{n+1} - \frac{n+1}{a} \mathrm{RHS}_n \\ &= \frac{e^{az}}{a} z^{n+1} - \frac{n+1}{a} I_n \qquad \text{since it is true for } n \\ &= \frac{e^{az}}{a} z^{n+1} - \frac{n+1}{a} \int e^{az} z^n dz \\ &= \frac{e^{az}}{a} z^{n+1} - \frac{n+1}{a} \left[e^{az} \frac{z^{n+1}}{n+1} - \int a e^{az} \frac{z^{n+1}}{n+1} dz \right] \\ &= \frac{e^{az}}{a} z^{n+1} - \frac{1}{a} e^{az} z^{n+1} + I_{n+1} \\ &= I_{n+1} \end{aligned}$$

It is thus true for all n by induction.

14.2 Integrals of the form $T_n(r) \equiv \int e^{az} z^n \ln z dz$

T_{-1}

$$\begin{aligned}
\int e^{az} \ln z \frac{1}{z} dz &= \ln z \int \frac{e^{az}}{z} dz - \int \frac{1}{z} \int \frac{e^{az}}{z} dz dz \\
&= \mathrm{Ei}(az) \ln z - \int \frac{\mathrm{Ei}(az)}{z} dz \\
&= \mathrm{Ei}(az) \ln z - \int \frac{1}{z} \left(\gamma + \ln az + \sum_{n=1}^{\infty} \frac{(az)^n}{n!n} \right) dz \qquad \text{[15](eq.5.1.10)} \\
&= \mathrm{Ei}(az) \ln z - \int \frac{\gamma}{z} dz - \int \frac{\ln az}{z} dz - \sum_{n=1}^{\infty} \frac{a^n}{n!n} \int z^{n-1} dz \\
&= \mathrm{Ei}(az) \ln z - \gamma \ln z - \frac{1}{2} \ln^2 az - \sum_{n=1}^{\infty} \frac{(az)^n}{n!n^2}
\end{aligned}$$

T_0

$$\begin{aligned}
T_0 &= \int e^{az} ln z dz \\
&= \frac{1}{a} e^{az} \ln z - \int \frac{1}{a} e^{az} \frac{1}{z} dz \\
&= \frac{e^{az}}{a} \ln z - \frac{\mathrm{Ei}(az)}{a} \\
&= \frac{1}{a} \left(e^{az} \ln z - \mathrm{Ei}(az) \right)
\end{aligned}$$

T_n , $n \geq 1$

$$\begin{aligned}
\int e^{az} \ln z z^n dz &= \ln z \int e^{az} z^n dz - \int \frac{1}{z} \int e^{az} z^n dz dz \\
&= \ln z \frac{e^{az}}{a^{n+1}} n! (-1)^n \sum_{k=0}^{n} \frac{(-az)^k}{k!} - \int \frac{1}{z} \frac{e^{az}}{a^{n+1}} n! (-1)^n \sum_{k=0}^{n} \frac{(-az)^k}{k!} dz \\
&= \ln z \frac{e^{az}}{a^{n+1}} n! (-1)^n \sum_{k=0}^{n} \frac{(-az)^k}{k!} - \frac{n!(-1)^n}{a^{n+1}} \sum_{k=0}^{n} \frac{(-a)^k}{k!} \int e^{az} z^{k-1} dz \\
&= \ln z \frac{e^{az}}{a^{n+1}} n! (-1)^n \sum_{k=0}^{n} \frac{(-az)^k}{k!} \\
&\quad - \frac{n!(-1)^n}{a^{n+1}} \left(\int \frac{e^{az}}{z} dz + \sum_{k=1}^{n} \frac{(-a)^k}{k!} \int e^{az} z^{k-1} dz \right) \\
&= \ln z \frac{e^{az}}{a^{n+1}} n! (-1)^n \sum_{k=0}^{n} \frac{(-az)^k}{k!} \\
&\quad - \frac{n!(-1)^n}{a^{n+1}} \left(\mathrm{Ei}(az) + \sum_{k=1}^{n} \frac{(-a)^k}{k!} \frac{e^{az}}{a^k} (k-1)! (-1)^{k-1} \sum_{j=0}^{k-1} \frac{(-az)^j}{j!} \right) \\
&= \ln z \frac{e^{az}}{a^{n+1}} n! (-1)^n \sum_{k=0}^{n} \frac{(-az)^k}{k!}
\end{aligned}$$

$$-\frac{n!(-1)^n}{a^{n+1}}\left(\mathrm{Ei}(az)-\sum_{k=1}^{n}\frac{e^{az}}{k}\sum_{j=0}^{k-1}\frac{(-az)^j}{j!}\right)$$

T_{2n-1}

$$\begin{aligned}T_{2n-1} &= -\ln z\frac{e^{az}}{a^{2n}}(2n-1)!\sum_{k=0}^{2n-1}\frac{(-az)^k}{k!}\\ &\quad+\frac{(2n-1)!}{a^{2n}}\left(\mathrm{Ei}(az)-\sum_{k=1}^{2n-1}\frac{e^{az}}{k}\sum_{j=0}^{k-1}\frac{(-az)^j}{j!}\right)\end{aligned}$$

14.3 Integrals of the form $\check{I}(\mu,\nu,r) \equiv \int I_m(\mu r)e^{\nu r}dr$.

$\check{I}_m(\mu,\nu,r)$, $m \neq 0$

$$\begin{aligned}\check{I}(\mu,\nu,r) &\equiv \int^r I_m(\mu r)e^{\nu r}dr \\ &= \frac{e^{\nu r}}{\nu}I_m - \frac{\mu}{\nu}\int^r I'_m e^{\nu r}dr \\ &= \frac{e^{\nu r}}{\nu}I_m - \frac{\mu}{2\nu}\left(\check{I}_{m+1} + \check{I}_{m-1}\right)\end{aligned}$$

This can be re-arranged in the form of a recursion relation as,

$$\check{I}_m = \frac{2}{\mu}e^{\nu r}I_{m-1} - \frac{2\nu}{\mu}\check{I}_{m-1} - \check{I}_{m-2}$$

$\check{I}_0(\mu,\nu,r)$, $\nu \neq 0$

$$\begin{aligned}\check{I}_0(\mu,\nu,r) &\equiv \int I_0(\mu r)e^{\nu r}dr \\ &= \frac{1}{\mu}\int e^{az}I_0(z)dz \quad \text{putting } z = \mu r \text{ and } a = \nu/\mu \\ &= \frac{1}{\mu}\int e^{az}\sum_{n=0}^{\infty}\frac{z^{2n}}{2^{2n}(n!)^2}dz \quad \text{from A \& S 9.6.12} \\ &= \frac{1}{\mu}\sum_{n=0}^{\infty}\frac{1}{2^{2n}(n!)^2}\int e^{az}z^{2n}dz \\ &= \frac{1}{\mu}\sum_{n=0}^{\infty}\frac{1}{2^{2n}(n!)^2}\frac{e^{az}(-1)^{2n}(2n)!}{a^{2n+1}}\sum_{k=0}^{2n}\frac{(-az)^k}{k!} \\ &= \frac{e^{\nu r}}{\nu}\sum_{n=0}^{\infty}\frac{(2n)!}{(n!)^2}\left(\frac{\mu}{2\nu}\right)^{2n}\sum_{k=0}^{2n}\left(-\frac{\nu}{\mu}z\right)^k\frac{1}{k!}\end{aligned}$$

$\check{I}_0(\mu,0,r)$

$$\begin{aligned}\check{I}_0(\mu,0,r) &= \int I_0(\mu r)dr \\ &= \frac{1}{\mu}\int I_0(z)dz \quad \text{putting } z = \mu r \\ &= \frac{1}{\mu}\int\sum_{n=0}^{\infty}\frac{z^{2n}}{2^{2n}(n!)^2}dz \\ &= \frac{1}{\mu}\sum_{n=0}^{\infty}\frac{z^{2n+1}}{(2n+1)2^{2n}(n!)^2} \\ &= \frac{1}{\mu}\sum_{n=0}^{\infty}\frac{(\mu r)^{2n+1}}{(2n+1)2^{2n}(n!)^2} \\ &= r\sum_{n=0}^{\infty}\frac{(\mu r/2)^{2n}}{(2n+1)(n!)^2}\end{aligned}$$

$\check{I}_1(\mu,\nu,r)$ Taking the $m=1$ case of the recursion relation we get;

$$\check{I}_1 = \frac{2}{\mu}e^{\nu r}I_0 - \frac{2\nu}{\mu}\check{I}_0 - \check{I}_{-1}$$

which, noting that $I_m = I_{-m}$ and hence $\check{I}_m = \check{I}_{-m}$, reduces to;

$$\check{I}_1 = \frac{e^{\nu r}}{\mu}I_0 - \frac{\nu}{\mu}\check{I}_0$$

14.4 Integrals of the form $\check{K}(\mu,\nu,r) \equiv \int K_m(\mu r)e^{\nu r}dr$.

$\check{K}_m(\mu,\nu,r)$, $m \neq 2$

$$\begin{aligned}\check{K}(\mu,\nu,r) &\equiv \int^r K_m(\mu r)e^{\nu r}dr \\ &= \frac{e^{\nu r}}{\nu}K_m - \frac{\mu}{\nu}\int^r K'_m e^{\nu r}dr \\ &= \frac{e^{\nu r}}{\nu}K_m + \frac{\mu}{2\nu}\left(\check{K}_{m+1} + \check{K}_{m-1}\right)\end{aligned}$$

This can be re-arranged in the form of a recursion relation as,

$$\check{K}_m = -\frac{2}{\mu}e^{\nu r}K_{m-1} + \frac{2\nu}{\mu}\check{K}_{m-1} - \check{K}_{m-2}$$

$\check{K}_0(\mu,\nu,r)$, $\nu \neq 0$ Proceeding for the K_0 Bessel function, we have (from [15](eq.9.6.12)),

$$\begin{aligned}\check{K}_0(\mu,\nu,r) &= \int e^{\nu r}K_0(\mu r)dr \\ &= \int e^{az}K_0(z)dz \quad \text{putting } z=\mu r \text{ and } a=\nu/\mu \\ \mu\check{K}(\mu,\nu,r) &= \int e^{az}\Big(-\Big(ln\frac{z}{2}+\gamma\Big)I_0(z) \\ &\quad + \sum_{n=1}^{\infty}\Big(1+\frac{1}{2}+\frac{1}{3}+\cdots+\frac{1}{n}\Big)\frac{z^{2n}}{2^{2n}(n!)^2}\Big)dz \\ &= \int e^{az}\Big\{(\ln 2 - \ln z - \gamma)\sum_{n=0}^{\infty}\frac{z^{2n}}{2^{2n}(n!)^2} \\ &\quad + \sum_{n=1}^{\infty}(\psi(n+1)-\gamma)\frac{z^{2n}}{2^{2n}(n!)^2}\Big)dz \\ &= \int e^{az}\Big((\ln 2 - \ln z - \gamma) + \sum_{n=0}^{\infty}\frac{z^{2n}}{2^{2n}(n!)^2}(\ln 2 - \ln z + \psi(n+1))\Big)dz\end{aligned}$$

$\check{K}_0(\mu,0,r)$

$$\check{K}_0(\mu,0,r) = \int K_0(\mu r)dr$$

$$
\begin{aligned}
&= \frac{1}{\mu}\int K_0(z)dz \qquad \text{putting } z = \mu r \\
&= \frac{1}{\mu}\Big(-\Big(\gamma + \ln\frac{z}{2}\Big) z \sum_{k=0}^{\infty} \frac{(z/2)^{2k}}{(k!)^2(2k+1)} \\
&\quad + z\sum_{k=0}^{\infty} \frac{(z/2)^{2k}}{(k!)^2(2k+1)^2} \\
&\quad + z\sum_{k=1}^{\infty} \frac{(z/2)^{2k}}{(k!)^2(2k+1)}\Big(1+\frac{1}{2}+\cdots+\frac{1}{k}\Big)\Big) \qquad \text{A. \& S. 11.1.9} \\
&= r\sum_{k=0}^{\infty} \frac{(z/2)^2 k}{(k!)^2(2k+1)}\Big(\psi(k+1) - \ln\frac{z}{2} + \frac{1}{2k+1}\Big)
\end{aligned}
$$

$\check{K}_1(\mu,\nu,r)$ Taking the $m = 1$ case of the previous recursion relation we get;

$$\check{K}_1 = \frac{2}{\mu}e^{\nu r}K_0 - \frac{2\nu}{\mu}\check{K}_0 - \check{K}_{-1}$$

which, noting that $K_m = K_{-m}$ and hence $\check{K}_m = \check{K}_{-m}$, reduces to;

$$\check{K}_1 = -\frac{e^{\nu r}}{\mu}K_0 + \frac{\nu}{\mu}\check{K}_0$$

14.5 Integrals of the form $\hat{K}(\mu,\nu,r) \equiv \int \frac{1}{r} K_m(\mu r) e^{\nu r} dr$

$\hat{K}_0(\mu,0,r)$

$$\begin{aligned}
\hat{K}_0(\mu,0,r) &\equiv \int \frac{1}{r} K_0(\mu,r) dr \\
&= -\int_r^\infty \frac{1}{r} K_0(\mu r) dr && \text{since we are free to choose the integration constant} \\
&= -\int_z^\infty \frac{1}{r} K_0(z) dz && \text{putting } z = \mu r
\end{aligned}$$

Using the expansion from [15](eq.11.1.22) this becomes;

$$\hat{K}_0(\mu,0,r) = -\frac{1}{2}\ln^2\frac{z}{2} - \gamma \ln\frac{z}{2} - \frac{\pi^2}{24} - \frac{\gamma^2}{2} + \sum_{k=1}^{\infty} \frac{(z/2)^{2k}}{2k(k!)^2}\left(\psi(k+1) + \frac{1}{2k} - \ln\frac{z}{2}\right)$$

where the *digamma* function ψ is given in [15](eq.6.3.2) as;

$$\psi(n) = \begin{cases} -\gamma & \text{when } n = 1 \\ -\gamma + \sum_{k=1}^{n-1} \frac{1}{k} & \text{when } n \geq 2 \end{cases}$$

and Euler's constant γ is;

$$\gamma \approx 0.5772156649$$

$\hat{K}_m(\mu,\nu,r)$, $m \neq 0$

$$\begin{aligned}
\hat{K}_m(\mu,\nu,r) &\equiv \int \frac{1}{r} K_m(\mu r) e^{\nu r} dr \\
&= \mu \int \frac{1}{\mu r} K_m(\mu r) e^{\nu r} dr \\
&= \mu \int \frac{-1}{2m} \left(K_{m-1}(\mu r) - K_{m+1}(\mu r)\right) e^{\nu r} dr && \text{using [15](eq.9.6.26)} \\
&= -\frac{\mu}{2m}\left(\check{K}_{m-1}(\mu,\nu,r) - \check{K}_{m+1}(\mu,\nu,r)\right) \\
&= -\frac{\mu}{2m}\left(\check{K}_{m-1} + \frac{2}{\mu} e^{\nu r} K_m - 2\frac{\nu}{\mu}\check{K}_m + \check{K}_{m-1}\right) \\
&= -\frac{1}{m}\left(\mu \check{K}_{m-1}(\mu,\nu,r) + e^{\nu r} K_m(\mu r) - \nu \check{K}_m(\mu,\nu,r)\right)
\end{aligned}$$

Where the recursion relation for the $\check{K}$'s was used in the 5'th line.

$\hat{K}_0(\mu,\nu,r)$, $\nu \neq 0$

$$\begin{aligned}
\hat{K}_0(\mu,\nu,r) &\equiv \int \frac{1}{r} K_0(\mu r) e^{\nu r} dr \\
&= \int \frac{1}{z} K_0(z) e^{az} dz && \text{,putting } z = \mu r \text{ and } a = \nu/\mu \\
&= \int \frac{e^{az}}{z}\left(-(\ln\frac{z}{2} + \gamma) I_0(z) + \sum_{n=1}^{\infty} \frac{z^{2n}}{2^{2n}(n!)^2}\left(1 + \frac{1}{2} + \frac{1}{3}\right)\right) dz && \text{[15](eq.9.6.13)} \\
&= \int \frac{e^{az}}{z}\left(-(\ln z - \ln 2 + \gamma) I_0(z) + \sum_{n=1}^{\infty} \frac{z^{2n}}{2^{2n}(n!)^2}\left(\psi(n+1) - \gamma\right)\right) dz
\end{aligned}$$

substituting the power series for I_0 from [15](eq.9.6.12) we get;

$$\begin{aligned}
\hat{K}_0(\mu,\nu,r) &= \int \frac{e^{az}}{z}\left(-(\ln z - \ln 2 + \gamma)\sum_{n=0}^{\infty}\frac{z^{2n}}{2^{2n}(n!)^2} + \sum_{n=1}^{\infty}\frac{z^{2n}}{2^{2n}(n!)^2}(\psi(n+1)-\gamma)\right)dz \\
&= \int \frac{e^{az}}{z}\left(\ln 2 - \ln z - \gamma + \sum_{n=1}^{\infty}\frac{z^{2n}}{2^{2n}(n!)^2}(\psi(n+1)+\ln 2 - \ln z)\right)dz \\
&= (\ln 2-\gamma)\mathrm{Ei}(az) - \int \frac{1}{z}e^{az}\ln z dz \\
&\quad + \sum_{n=1}^{\infty}\frac{1}{2^{2n}(n!)^2}\left((\psi(n+1)+\ln 2)\int e^{az}z^{2n-1}dz - \int e^{az}z^{2n-1}\ln z dz\right) \\
&= (\ln 2-\gamma)\mathrm{Ei}(az) - T_{-1} \\
&\quad + \sum_{n=1}^{\infty}\frac{1}{2^{2n}(n!)^2}\left(-T_{2n+1} - (\psi(n+1)+\ln 2)(2n-1)!\frac{e^{az}}{a^{2n}}\sum_{k=0}^{2n-1}\frac{(-az)^k}{k!}\right) \\
&= (\ln 2-\gamma)\mathrm{Ei}(az) - T_{-1} \\
&\quad - \sum_{n=1}^{\infty}\frac{1}{2^{2n}(n!)^2}\left(T_{2n+1} - (\psi(n+1)+\ln 2)(2n-1)!\frac{e^{az}}{a^{2n}}\sum_{k=0}^{2n-1}\frac{(-az)^k}{k!}\right)
\end{aligned}$$

where we define the terms T_n by;

$$T_n = \int e^{az}z^n \ln z dz$$

14.6 Integrals of the form $\hat{I}(\mu,\nu,r) \equiv \int \frac{1}{r} I_m(\mu r) e^{\nu r} dr$.

$\hat{I}_0(\mu,0,r)$

$$\begin{aligned}
\hat{I}_0(\mu,0,r) &= \int \frac{1}{r} I_0(\mu r) dr \\
&= \int \frac{1}{z} I_0(z) dz \qquad \text{putting } z = \mu r \\
&= \int \frac{1}{z} \sum_{n=0}^{\infty} \frac{z^{2n}}{2^{2n}(n!)^2} dz \qquad \text{using [15](eq.9.6.12)} \\
&= \sum_{n=0}^{\infty} \int \frac{z^{2n-1}}{2^{2n}(n!)^2} dz \\
&= \int \frac{dz}{z} + \sum_{n=1}^{\infty} \int \frac{z^{2n}}{2^{2n}(n!)^2} dz \\
&= \ln z + \frac{1}{2} \sum_{n=1}^{\infty} \frac{(z/2)^{2n}}{n(n!)^2}
\end{aligned}$$

$\hat{I}_m(\mu,\nu,r)$, $m \neq 0$

$$\begin{aligned}
\hat{I}_m(\mu,\nu,r) &\equiv \int \frac{1}{r} I_m(\mu r) e^{\nu r} dr \\
&= \mu \int \frac{1}{\mu r} I_m(\mu r) e^{\nu r} dr \\
&= \mu \int \frac{1}{2m} \left(I_{m-1}(\mu r) - I_{m+1}(\mu r) \right) e^{\nu r} dr \qquad \text{using [15](eq.9.6.26)} \\
&= \frac{\mu}{2m} \left(\check{I}_{m-1}(\mu,\nu,r) - \check{I}_{m+1}(\mu,\nu,r) \right) \\
&= \frac{\mu}{2m} \left(\check{I}_{m-1} - \frac{2}{\mu} e^{\nu r} I_m + 2\frac{\nu}{\mu} \check{I}_m + \check{I}_{m-1} \right) \\
&= \frac{1}{m} \left(\mu \check{I}_{m-1}(\mu,\nu,r) - e^{\nu r} I_m(\mu r) + \nu \check{I}_m(\mu,\nu,r) \right)
\end{aligned}$$

Where the recursion relation for the $\check{I}$'s was used in the 5'th line.

$\hat{I}_0(\mu,\nu,r)$, $\nu \neq 0$

$$\begin{aligned}
\hat{I}_0(\mu,\nu,r) &\equiv \int \frac{1}{r} I_0(\mu r) e^{\nu r} dr \\
&= \int \frac{1}{r} e^{\nu z} \sum_{n=0}^{\infty} \frac{(\mu r)^2 n}{2^{2n}(n!)^2} dz \qquad \text{using [15](eq.9.6.12)} \\
&= \int e^{az} \sum_{n=0}^{\infty} \frac{z^{2n-1}}{2^{2n}(n!)^2} dz \qquad \text{putting } z = \mu r \text{ and } a = \nu/\mu \\
&= \sum_{n=0}^{\infty} \frac{1}{2^{2n}(n!)^2} \int e^{az} z^{2n-1} dz \\
&= \int \frac{e^{az}}{z} dz - \sum_{n=1}^{\infty} \frac{(2n-1)!}{2^{2n}(n!)^2} \frac{e^{az}}{a^{2n}} \sum_{k=0}^{2n-1} \frac{(-az)^k}{k!}
\end{aligned}$$

$$= \mathrm{Ei}(az) - e^{az} \sum_{n=1}^{\infty} \frac{(2n-1)!}{(2a)^{2n}(n!)^2} \sum_{k=0}^{2n-1} \frac{(-az)^k}{k!}$$

$$= \mathrm{Ei}(\nu r) - e^{\nu r} \sum_{n=1}^{\infty} \left(\frac{\mu}{2\nu}\right)^{2n} \frac{(2n-1)!}{(n!)^2} \sum_{k=0}^{2n-1} \frac{(-\nu r)^k}{k!}$$

References

[1] S. Puri *Role of plasma equilibrium current in Alfvén wave antenna optimization* Nuclear Fusion, Vol.27, No.7 (1987)

[2] S. Puri *Antenna optimization for Alfvén wave heating* Nuclear Fusion, Vol.27, No.2 (1987)

[3] K. Theilhaber, J. Jacquinot *Variational theory of the ICRH antenna* Nuclear Fusion, Vol.24, No.5, (1984)

[4] S. Puri *Self-consistent, analytic, periodic-loop antenna theory* Physics of Fluids, **27** (8), August 1984

[5] G. Cattanei, A. B. Murphy *Dependence of heating efficiency and impurity production on the toroidal wavelength in ion cyclotron resonance heating* Nuclear Fusion, Vol.31, No.2 (1991)

[6] G. L. Chen et. al. *A 3-D analysis of arbitarily shaped antennas and Faraday shields* 13th Europen Conf on Controlled Fusion and Plasma Heating, Vol.10C, Part II, p101

[7] D. W. Faulconer et. al. *Method for rapid evaluation of antenna near-fields* 13th Europen Conf on Controlled Fusion and Plasma Heating, Vol.10C, Part II, p69

[8] A. M. Messiaen et. al. *Analysis of the plasma edge radiation by ICRH antenna* Proc. of the 4'th Intl. Symp. on Heating in Toroidal plasmas Rome 1984, Vol.1, p315

[9] V. P. Bhatnagar et. al. *Comprehensive analysis of antenna-plasma coupling in ICR heating of tokamaks and study of energy deposition* Plasma Physics and Contrl. Nuc. Fus. Research, 1982, Vol.II, IAEA-CN-41/J-2, p103

[10] Warren L. Stutzman and Gary A. Theile *Antenna Theory and Design*, Book published 1981 by John Wiley & Sons, Inc.

[11] Fink and Christianson *Electronics Engineers' Handbook - Second Edition*, Published by Mc Graw Hill.

[12] M. Brambilla *Impedance Matrix Formalism for the self-consistent modelling of loop antennas in the ion-cyclotron frequency range* Max-Planck-Institut fur Plasmaphysik internal report IPP 5/45 March 1992.

[13] M. Ballico and H. Lederer *PVM on ALPHA AXP Workstations in a Customer Applications Environment*, Max-Planck-Institut fur Plasmaphysik internal report IPP R/45 Sept 1993.

[14] D. G. Swanson *Plasma Waves* Academic Press Inc. 1989.

[15] M. Abramowitz and I. A. Stegun *Handbook of Mathematical functions* Dover Publications, Inc., New York, Dec. 1972.

[16] F. B. Hildebrand *Advanced Calculus for Applications* Book, Prentice-Hall, Inc. 1976.

[17] V. P. Bhatnagar & J. Jacquinot *A wide-band antenna for the NEXT-STEP Tokamak* JET-P(93)76 Internal JET report 6/10/93.